applied sciences

MDPI

Review

Cutaneous Thermography in the Diagnosis and Management of Arthropathies: Pathophysiology, Diagnostic Pathways, and Multimodal Imaging Correlations

Constantin-Adrian Andrei [1,2], Serban Dragosloveanu [1,2,*], Alex-Gabriel Grigore [2], Iosif-Aliodor Timofticiuc [1], Rares-Mircea Birlutiu [1,2], Catalin Anghel [3], Adelina-Elena Moise [1,2], Mihai Emanuel Gherghe [1,2], Łukasz Pulik [4], Adrian Iftime [1], Romica Cergan [1,2], Constantin Caruntu [1,5] and Cristian Scheau [1,2]

1 Faculty of Medicine, The "Carol Davila" University of Medicine and Pharmacy, 050474 Bucharest, Romania; constantin-adrian.andrei@drd.umfcd.ro (C.-A.A.); iosif-aliodor.timofticiuc2022@stud.umfcd.ro (I.-A.T.); raresmircea@gmail.com (R.-M.B.); adelina-elena.moise@drd.umfcd.ro (A.-E.M.); mihai-emanuel.gherghe@drd.umfcd.ro (M.E.G.); adrian.iftime@umfcd.ro (A.I.); r.cergan@gmail.com (R.C.); costin.caruntu@gmail.com (C.C.); cristian.scheau@umfcd.ro (C.S.)

2 "Foisor" Clinical Hospital of Orthopaedics, Traumatology and Osteoarticular TB, 021382 Bucharest, Romania; alexgrigore01@gmail.com

3 Department of Computer Science and Information Technology, "Dunărea de Jos" University of Galati, 800146 Galati, Romania; catalin.anghel@ugal.ro

4 Department of Orthopedics and Traumatology, Medical University of Warsaw, 02-005 Warsaw, Poland; lukasz.pulik@wum.edu.pl

5 Department of Dermatology, "Prof. N.C. Paulescu" National Institute of Diabetes, Nutrition and Metabolic Diseases, 011233 Bucharest, Romania

* Correspondence: serban.dragosloveanu@umfcd.ro

Abstract

Background: Arthropathies are a substantial source of global morbidity and healthcare costs, and there is a clinical need for accessible tools capable of detecting inflammatory and metabolic changes beyond conventional structural imaging. This review consolidates the recent evidence on infrared thermography (IRT) as a diagnostic and monitoring adjunct in the major arthropathies. **Methods**: A structured narrative review was conducted. A literature search of PubMed, Web of Science Core Collection, and Scopus was performed to identify relevant studies published between January 2016 and December 2025 using thermography- and arthropathy-related keywords and controlled-vocabulary terms combined with Boolean operators; only original full-text studies in English published within the previous decade were eligible. The structured search yielded 53 primary studies. Additional sources, including narrative and systematic reviews, methodological references, and book chapters, were drawn upon to inform the Introduction, Discussion, and interpretation but were not included in the primary evidence synthesis. **Results**: Across the included studies, IRT detected clinically meaningful thermal changes in most cases of osteoarthritis, rheumatoid arthritis, juvenile idiopathic arthritis, Charcot neuroarthropathy, and post-arthroplasty states, with thermal signals correlating moderately with ultrasound-detected synovitis, inflammatory biomarkers, and symptom distribution. **Discussion**: The evidence base is heterogeneous, however: temperature distributions overlap substantially between patients and controls, well-conducted negative results exist for hand thermography in low-activity rheumatoid arthritis, and reported effect sizes vary widely across devices and protocols. Quantitative thermographic metrics and machine-learning approaches may further refine diagnostic performance and enable remote monitoring. **Conclusions**: IRT is a promising rapid, non-invasive, radiation-free adjunctive imaging modality, but its clinical adoption is constrained by methodological variability, environmental and vascular

Academic Editors: Rodrigo Martín-San Agustín, Adrián Escriche Escuder and Iván J. Fuentes Abolafio

Received: 17 April 2026
Revised: 29 May 2026
Accepted: 3 June 2026
Published: 5 June 2026

confounders, and the absence of prospective validation. Standardised acquisition protocols and prospective multi-site validation are required before routine clinical use.

Keywords: infrared thermography; thermal physiology; tissue perfusion; functional recovery; joint inflammation; arthropathies; cutaneous temperature gradients; personalized rehabilitation; quantitative thermography; musculoskeletal diagnostics

1. Introduction

Arthropathies are major contributors to global morbidity and imply high healthcare costs. Osteoarthritis (OA), especially in the knee, is increasingly common, affecting over 5.5% of the population and accounting for more than 606 million cases in 2021 [1,2]. OA mainly affects adults over 40 years old, with over 20% in this group experiencing symptoms caused by cartilage damage and knee inflammation [3]. Rheumatoid arthritis alone affected approximately 17.6 million people globally, and was responsible for approximately 3.06 million disability-adjusted life-years, showing its substantial contribution to global disability [2]. Psoriatic arthritis (PsA) is often underdiagnosed but affects 112 per 100,000 adults globally, with higher rates in Europe and North America, and about 37 per 100,000 in Asia [4]. Septic arthritis occurs in 4–29 per 100,000 people and can cause permanent joint damage and systemic infection if not treated promptly [5].

Radiographs are typically the first-line test for joint assessment due to their ease of access and capacity to visualize bony structures [6,7]. However, they demonstrate limitations in the detection of early cartilage or soft tissue changes and may omit signs of active disease [8]. Magnetic resonance imaging (MRI) provides high-resolution images of these structures, but it is more expensive, time-consuming, and still shows limited accessibility in specific areas and populations [9]. Advanced MRI techniques for cartilage evaluation are primarily used in research [10]. Ultrasound is effective for identifying synovial thickening and blood flow, but requires skilled operators and is less effective for deeper joints such as the hip [11]. Currently, no bedside tool offers sensitivity to inflammation while being portable, safe, and affordable. There is a clinical need for adjunct techniques that can detect metabolic and vascular changes earlier than structural imaging.

Raised tissue temperature, or calor, was first identified by Celsus as a key sign of inflammation, resulting from vasodilation, increased blood flow, and elevated metabolic activity [12]. In joint diseases, synovial inflammation leads to angiogenesis and leucocyte accumulation, therefore generating heat perceivable at the skin surface [13,14]. Measuring the released heat can help differentiate disease types and guide treatment [15]. Infrared thermography (IRT) converts infrared radiation into digital temperature maps, with modern infrared cameras being able to detect subtle cutaneous temperature differences [3]. However, their thermal sensitivity depends on the detector, optics, calibration, acquisition distance, software processing, and environmental control [3,16,17]. Therefore, sensitivity values should be interpreted as device- and protocol-specific rather than as a universal characteristic of IRT [3]. Studies show that individuals with more severe knee OA or lateral knee pain show higher knee temperatures compared to healthy controls, particularly in specific regions such as the patellar region, popliteal fossa, or medial compartment [16,18]. These thermal patterns may also be influenced by underlying biomechanical factors such as coronal plane alignment, as osteoarthritic knees frequently exhibit varus deformity and altered joint loading patterns [19]. Occupational muscle strain can also increase skin temperature; for example, thermal imaging of dentists (a FLIR B200 thermal camera was used to monitor dentists at four time points—baseline, 15 min, 30 min of work, and post-stretching)

showed elevated temperatures in the neck, arms, and lower back during prolonged work, which decreased after stretching [18].

IRT is non-invasive, radiation-free, passive, and relatively affordable, rendering it suitable for bedside use [20]. Modern thermal cameras capture clear images and offer quantitative data, supporting ongoing monitoring [21]. Studies have found that IRT is simple, accurate, and safe, offering information on heat, metabolism, and blood flow, and can be used for screening, diagnosis, and follow-up [18,22]. In orthopaedics, a scoping review of 43 studies demonstrated the use of IRT in arthritis, Charcot foot, postoperative joint infections, carpal tunnel syndrome, sports injuries, and spine disorders, reflex sympathetic dystrophy, and diabetic foot infections [23]. IRT has also been promoted as a tool for evaluating musculoskeletal strain [21].

Recent studies and reviews have established a strong evidence base for the use of cutaneous thermography in arthropathies. Vardasca et al. reviewed 33 studies on arm and forearm thermography, concluding that IRT provides physiological information and has potential across musculoskeletal disorders [22]. Schiavon et al.'s review of inflammatory and degenerative joint diseases found IRT to be simple, accurate, and non-invasive, with increasing interest in temperature data such as ΔT, Hot-Dot Index, and ThermoJIS for phenotyping [21]. De Marziani et al. found that symptomatic knees in bilateral knee OA have higher temperatures than asymptomatic contralateral knees, particularly in the medial region [3]. Collectively, these studies support the growing evidence base and the need for methodological standardization and integration with multimodal imaging: radiography (for Kellgren–Lawrence grading) [24,25], MRI (for cartilage and synovitis) [26], and ultrasound (for effusion and synovitis) [27], which positions IRT as a complementary tool.

Several recent reviews have addressed IRT in joint disease, including the systematic review by Schiavon et al. on inflammatory and degenerative joint diseases [21], the systematic review by Vardasca et al. of arm and forearm musculoskeletal applications [22], and the orthopaedic-focused review by Kumar et al. [23]. The present review is distinct in two specific respects. First, it consolidates the disease-specific diagnostic role of IRT across the main arthropathies, osteoarthritis, rheumatoid arthritis, juvenile idiopathic arthritis, Charcot neuroarthropathy, and post-arthroplasty states, in a single framework, drawing together evidence that is otherwise distributed across modality- and disease-specific reviews. Second, it proposes an explicit, conceptual diagnostic and monitoring workflow that locates IRT relative to ultrasound, MRI, and laboratory testing, identifying where it is plausibly additive in routine care and where the evidence does not yet support its use. The pathophysiological and pattern-description content of the review draws on the prior reviews where appropriate and is presented in condensed form to keep the focus on these two contributions.

This review summarizes the evidence on IRT for the diagnosis and monitoring of arthropathies during the past decade, with emphasis on the physiological basis, technical standards, and relevant metrics. An assessment of clinical applications and limitations is also provided, along with a roadmap for integrating thermography into multimodal care in rehabilitation medicine, rheumatology, and orthopedics.

2. Materials and Methods

2.1. Study Design

This study was structured as a narrative review with a systematic identification of the literature, designed to synthesize current evidence regarding the role of cutaneous infrared thermography in the diagnosis, monitoring, and management of arthropathies. The methodology follows the PRISMA 2020 statement to maximize transparency and reproducibility. In this review, we aim to cover the pathophysiological basis of thermal

changes in arthropathies, technical principles and standardization requirements of IRT, disease-specific thermographic patterns, and to describe the current use of IRT in OA, RA, JIA, Charcot neuroarthropathy and septic or infection-related joint disease, in order to highlight its utility as an adjunctive tool within a multimodal approach to diagnosis and monitoring.

The structured search was employed for the selection of the original clinical and computational studies for the evidence tables. Other additional reviews, systematic reviews, scoping reviews, book chapters, or methodological papers were kept if useful as background, for the technical description, historical information, or for providing interpreted value for the narrative synthesis.

2.2. Literature Search Strategy

An extensive search of the PubMed, Scopus, and Web of Science literature databases was performed with articles published from January 2016 to December 2025. The PubMed search string was: ("Thermography"[Mesh] OR "Infrared Rays"[Mesh] OR thermography[tiab] OR "infrared thermography"[tiab] OR "thermal imaging"[tiab] OR "infrared imaging"[tiab] OR "cutaneous thermography"[tiab] OR "skin temperature"[tiab]) AND ("Osteoarthritis"[Mesh] OR "Arthritis"[Mesh] OR osteoarthritis[tiab] OR arthritis[tiab] OR arthropathy[tiab] OR "joint inflammation"[tiab] OR "septic arthritis"[tiab] OR "periprosthetic joint infection"[tiab] OR "total knee arthroplasty"[tiab] OR "total hip arthroplasty"[tiab]) AND (diagnosis[tiab] OR diagnostic[tiab] OR monitoring[tiab] OR management[tiab] OR assessment[tiab] OR follow-up[tiab]) NOT (review[pt] OR systematic review[ti] OR meta-analysis[pt] OR scoping review[ti]) AND Humans[Mesh] AND English[lang]. The Scopus and Web of Science search strings were analogous, adjusted for respective databases (using title, abstract, and keywords). Supplementary search with review of reference lists of found literature, in particular, reviewing the bibliographies of previous relevant systematic reviews, provided additionally selected relevant references, but they were not included in the evidence tables and only used to support arguments within the main section of the review article. An extensive (yet select) search of older (non-primary) literature was made to find historically relevant articles, methodological details, or to complement findings based on evidence presented by the recent papers.

2.3. Eligibility Criteria

Included studies were those that focused on cutaneous/infrared/thermal imaging and any form of arthropathies or joint-related clinical conditions, providing outcome measures in relation to diagnosis, monitoring, management, postoperative follow-up, disease activity, or multimodal imaging correlations. Studies including any human participants or based on clinically relevant thermographic data were eligible, provided that full texts were accessible in English, original studies were published in between the specified search period, and included data suitable for evaluation.

Exclusion criteria included: studies that did not involve cutaneous/infrared thermography and/or arthropathies; those dealing solely with experimental or animal models, and no direct or indirect clinical relevance, as well as purely experimental or animal models of arthropathies, non-articular musculoskeletal disorders without specific mention of joint affection; incomplete data (lack of full-text availability, missing data); non-human subjects and duplicated studies with no additional information. Review articles, systematic reviews, meta-analyses, scoping reviews, editorial commentaries, letters, case reports, and book chapters were excluded from the main structured evidence table, although included to supplement background, technical description, or discussion if of added value.

2.4. Study Selection

All records identified were imported into a reference management software, and duplicates were excluded using automated features, followed by manual verification. There were 438 references identified during the search, including 438 references identified from the databases (PubMed, n = 58; Scopus, n = 235; Web of Science, n = 145). 145 duplicates were excluded after removal, followed by the exclusion of 15 conference proceedings, 5 book records, 3 retracted articles, and 9 literature reviews, resulting in 261 records ready for initial title and abstract screening.

Two independent reviewers performed title/abstract screening and full-text review of eligible records. From the records deemed relevant for full-text review, 152 records were removed because of clear irrelevance to the scope of the review. 109 full-text articles were assessed for relevance; 55 of which were excluded for predetermined reasons, including: absence of thermographic assessment, only indirectly related to arthropathies, used a different technology, full-text could not be found, non-human study, irrelevant outcomes in the context of a diagnostic or follow-up monitoring.

Ultimately, 53 original studies were selected for inclusion in the structured evidence table. Supplementary sources were selected to provide context for the Introduction, the technical details, the pathophysiological rationale, and the discussion, and are not counted within the 53 included studies. The title and abstract screening and the subsequent full-text relevance assessment was conducted by two separate reviewers, and inconsistencies resolved by discussion and consensus. The process of study selection is illustrated in Figure 1.

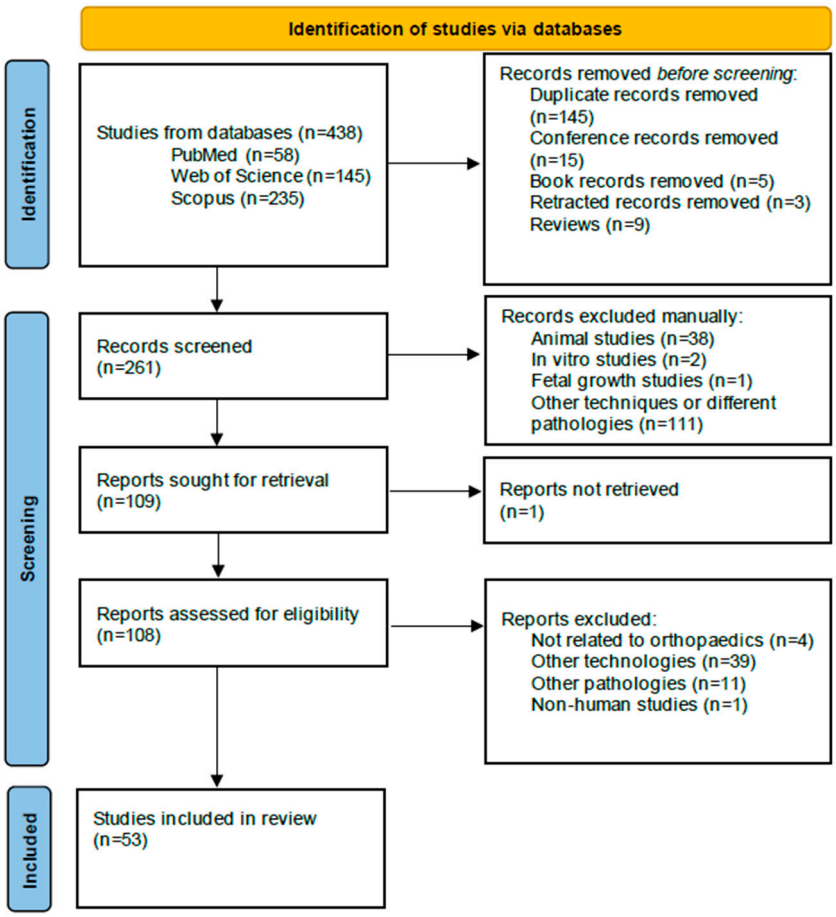

Figure 1. PRISMA flow diagram of literature search and study selection for thermography in arthropathies.

2.5. Data Extraction

All relevant information from included studies was extracted onto a structured template. Data extraction was conducted by a single reviewer, and verified by another independent reviewer. Extracted data included: study design, characteristics of patient population, sample size, type of arthropathy, anatomical region evaluated, infrared device and/or technology used, thermal acquisition protocol, controlled environmental conditions (if specified), description of regions of interest, thermographic parameters measured, reference method/comparator, main quantitative results and their significance (if stated), and the main study limitations.

Risk of Bias assessment was performed by one reviewer and verified by the other independently. Differences were resolved by discussion and consensus. Given the high heterogeneity of studies, a scoring tool was not used and the assessment was performed qualitatively. Main features of a good study design were based on study design, sample size and patient population selection criteria, definition of diagnoses used, thermographic device used and its specifications, thermographic parameters and standardization, environmental conditions controls, the definition of ROI, use of a comparator or gold standard, the completeness of clinical and thermal data obtained, and statistical significance of the results. Computational and machine learning studies were evaluated based on size of the dataset, computational method, segmentation method, validation strategy, model performance, and presence or absence of external validation. In the context of this review, the assessment of Risk of Bias was not used as an exclusion criterion but as a method of contextualization of the findings. Main limitation factors often observed among studies included the lack of adequate retrospective or longitudinal design, the relatively small sample size and variability of thermographic devices used, non-standardized room/acclimatization settings, inconsistent ROI definitions, incomplete reporting of environmental conditions, lack of external validation, and lack of diagnostic cut-offs and inconsistent measurement results.

A formal quantitative meta-analysis was considered but not performed. The included studies differed substantially in disease entity, affected anatomical region, thermographic device, acquisition protocol, ROI definition, and reported outcome metrics. The evidence is therefore presented as a narrative synthesis structured by disease entity and quantitative metric, with discussions of heterogeneity contextualized in each chapter.

3. Results

Infrared thermography is becoming a useful, non-invasive way to identify and monitor inflammation in various joint diseases. Due to data heterogeneity, retrieved studies have been split into 2 main categories. Henceforth, Tables 1 and 2 present the key ideas and findings of studies that addressed thermographic assessment from clinical and computational viewpoints and in different types of arthritis (rheumatoid arthritis, osteoarthritis, juvenile idiopathic arthritis, diabetic Charcot arthropathy, etc.).

Table 1. Clinical studies evaluating infrared thermography in arthropathies.

Study Design/Population	Condition/Joint	Device/ Protocol	Comparator/ Thermal Metric	Statistical Thermographic Result	Main Limitation	Refs
Single-center observational study; 30 patients undergoing arthrocentesis	Knee arthritis with effusion	FLIR ONE Pro smartphone camera (FLIR Systems, Inc., Wilsonville, OR, USA); 20 min rest; room 22 ± 1 °C; tripod at 1 m; circular anterior knee ROI (region of interest)	PDUS (power Doppler ultrasound), synovial WBC (white blood cell) count, blood inflammatory markers; Tmax (maximum temperature), Tmin (minimum temperature), Tave (average temperature), Tmax–Tmin	PDUS-positive knees were warmer than PDUS-negative knees: Tmax 33.2 vs. 30.5 °C, $p = 0.025$; Tmin 30.7 vs. 27.0 °C, $p = 0.015$; Tave 32.1 vs. 29.1 °C, $p = 0.016$; AUC (area under the curve) 0.764–0.790	Small heterogeneous cohort; only one smartphone device; synovial WBC did not correlate with IRT (infrared thermography)	[28]
Usability study; 11 knee OA (osteoarthritis) patients, 11 caregivers, 11 clinicians	Knee OA/remote monitoring	FLIR ONE Pro smartphone camera (FLIR Systems, Inc., Wilsonville, OR, USA); caregiver-acquired knee images through app-guided remote-monitoring platform	Usability questionnaires; highest temperature in selected knee ROI	No diagnostic thermographic difference tested; usability high: patients 10/10, caregivers 8.5/10; overall usability 8.7–8.8/10	Usability/acceptability only; no OA severity or diagnostic validation	[29]
Pilot study; 10 RA (rheumatoid arthritis) patients, 11 controls; compared with prior PsA (psoriatic arthritis) group	RA/dominant hand	High-resolution thermal imaging camera (manufacturer not reported); 20 dorsal hand ROIs; baseline and post-isometric exercise recovery imaging	Healthy controls, prior PsA cohort, qualitative PWD-US (power Doppler ultrasound); baseline/recovery temperature metrics	RA patients had lower thermal parameters than controls; all parameters except baseline slope differed significantly, $p < 0.025$	Very small cohort; ultrasound comparison qualitative; camera model not clearly reported	[30]
Cross-sectional study; 25 pathological hands, 15 healthy hands	Hand/wrist neuropathic and musculoskeletal disorders	FLIR E54 thermal camera (FLIR Systems, Inc., Wilsonville, OR, USA); dorsal/palmar views; 21 °C room; 15 min acclimatization; camera 0.7 m	Pathological vs. healthy hands; mean, maximum, and minimum temperatures across finger/wrist/forearm ROIs	Pathological hands were warmer than controls in dorsal and palmar views, $p < 0.01$; dorsal ΔT (temperature difference) ≈ 0.78–1.33 °C; palmar ΔT ≈ 0.71–3.49 °C	Heterogeneous pathology group; not arthropathy-specific; small sample	[31]
Reliability study; 30 diabetes-related Charcot neuroarthropathy patients analyzed	Charcot neuroarthropathy/foot and ankle	DermaTemp DT-1001 handheld infrared dermal thermometer (Exergen Corporation, Watertown, MA, USA); ≥15 min acclimatization; 10 anatomical foot/ankle sites; touch and non-touch techniques	Intra-/inter-rater reliability; site-specific dermal temperature	Good-to-excellent reliability: touch intra-rater ICC (intraclass correlation coefficient) 0.87–0.99, inter-rater ICC 0.83–0.98; non-touch intra-rater ICC 0.93–0.99, inter-rater ICC 0.91–0.99	Reliability study only; no diagnostic accuracy; thermometer rather than thermographic camera	[32]

Table 1. *Cont.*

Study Design/Population	Condition/Joint	Device/ Protocol	Comparator/ Thermal Metric	Statistical Thermographic Result	Main Limitation	Refs
Prospective clinical study; 60 symptomatic monolateral knee OA patients	Knee OA/symptomatic knee	FLIR T1020 thermal camera (FLIR Systems, Inc., Wilsonville, OR, USA); 1024 × 768 pixels; sensitivity 0.02 °C; 10 min thermalization; images at baseline, immediately after 2 min exercise, and 5 min after exercise	Time-point comparison; total knee and 5 ROIs: medial/lateral patella, suprapatellar, medial knee, lateral knee	Total knee temperature changed after exercise: 32.13 ± 1.07 °C at baseline, 31.86 ± 1.12 °C immediately after, 31.94 ± 1.10 °C at 5 min; $p = 0.002$	No healthy control; large interindividual variability; no US/MRI (ultrasound/magnetic resonance imaging) comparator	[33]
Within-patient comparative study; 66 bilateral knee OA patients with one symptomatic knee	Knee OA/symptomatic vs. asymptomatic knee	FLIR T1020 thermal camera (FLIR Systems, Inc., Wilsonville, OR, USA); 1024 × 768 pixels; sensitivity 0.02 °C; 10 min thermalization; anterior bilateral knee view	Symptomatic vs. contralateral knee; KL (Kellgren–Lawrence) grade; pain location; total and regional mean temperature	Symptomatic knees were warmer: total knee 31.9 ± 1.1 vs. 31.6 ± 1.1 °C, $p = 0.003$; medial ROI $p < 0.0005$; when KL grade was equal, medial ROI remained significant, $p = 0.037$	No ultrasound/MRI confirmation of inflammation; anterior view only	[3]
Comparative study; 31 RA patients in remission, 51 controls	RA/hands and wrists	FLIR T630 thermal camera (FLIR Systems, Inc., Wilsonville, OR, USA); 640 × 480 pixels; NETD (noise-equivalent temperature difference) < 23 mK; 20 min acclimatization; palmar and dorsal views	RA remission vs. controls; DAS28 (Disease Activity Score in 28 joints), CRP (C-reactive protein), Ritchie Articular Index; US subset	RA patients had warmer palms and fingers: palms 31.4 ± 1.84 vs. 29.37 ± 2.2 °C, $p = 0.001$; fingers 30.22 ± 2.4 vs. 27.16 ± 3.2 °C, $p = 0.001$	Age mismatch; not all RA patients had ultrasound; remission-pattern study	[34]
Comparative study; 32 RA remission patients, 51 controls	RA/feet	FLIR T630 thermal camera (FLIR Systems, Inc., Wilsonville, OR, USA); 640 × 480 pixels; ≥15 min acclimatization; plantar images; forefoot and heel ROIs	RA remission vs. controls; mean plantar ROI temperature	RA feet were warmer in all plantar ROIs: forefoot $p = 0.004$–0.005; heel $p \leq 0.002$	Age mismatch; ultrasound only in subset; not active synovitis validation	[35]
Comparative study; 81 RA patients, 39 controls	RA/rheumatoid foot and MTP (metatarsophalangeal) joints	ThermaCAM SC640 thermal camera (FLIR Systems, Inc., Wilsonville, OR, USA); emissivity 0.98; 20 min acclimatization; dorsal foot images; 7 manual ROIs	RA vs. controls; ultrasound-defined inflamed vs. non-inflamed MTP joints	RA patients had higher foot temperatures than controls in all ROIs, $p = 0.0000$–0.0001; US-positive MTP joints were not consistently warmer	Age mismatch; manual ROI placement; weak correspondence with US-defined inflammation	[36]

Table 1. *Cont.*

Study Design/Population	Condition/Joint	Device/ Protocol	Comparator/ Thermal Metric	Statistical Thermographic Result	Main Limitation	Refs
Prospective cohort; 49 suspected knee arthritis patients: 15 septic, 34 non-septic	Septic arthritis/knee	FLIR E75 thermal camera (FLIR Systems, Inc., Wilsonville, OR, USA); 320 × 240 pixels; sensitivity 0.03 °C; bilateral knee imaging with camera 20 cm above knees	Septic vs. non-septic arthritis; aspiration and culture; hottest, coldest, and average temperature differences	Septic arthritis showed greater average side-to-side ΔT: 3.40 ± 1.80 vs. 0.94 ± 1.16 °C, $p < 0.001$; affected-knee average temperature 37.10 vs. 35.89 °C, $p = 0.020$	Small cohort; IRT cannot replace aspiration/culture; limited differentiation from mimics	[37]
Active thermography study; 48 high-activity RA patients, 45 controls	RA/fingers and hands	FLIR E60bx thermal camera (FLIR Systems, Inc., Wilsonville, OR, USA); 320 × 240 pixels; sensitivity < 0.05 °C; cold-water provocation at 0 °C; 180 s rewarming	RA vs. controls; heating rate in °C/min for whole hand and proximal phalanges	Proximal-phalanx heating rates were significantly lower in RA than controls, $p < 0.05$; whole-hand mean heating rate lower but not significant	Dynamic provocation study; no ultrasound or biomarker comparator	[38]
Cross-sectional study; 49 RA patients, 30 controls	RA/MCP (metacarpophalangeal) and PIP (proximal interphalangeal) joints	FLIR T300 thermal camera (FLIR Systems, Inc., Wilsonville, OR, USA); NETD < 0.05 °C; 15 min rest; camera 0.5 m; standardized hand splint	RA vs. controls; DAS28, HAQ (Health Assessment Questionnaire), ESR (erythrocyte sedimentation rate), CRP; central spot and average box temperature	RA joints were warmer than controls: MCP coefficient +2.56 °C, $p < 0.001$; PIP coefficient +2.72 °C, $p < 0.001$; no useful association with DAS28, ESR, CRP, or HAQ	Age mismatch; no US/MRI comparator; limited value for activity assessment	[39]
Cross-sectional study; 46 JIA patients, 15 controls	JIA/wrist	FLIR E60 thermal camera (FLIR Systems, Inc., Wilsonville, OR, USA); sensitivity 0.045 °C; 15 min acclimatization; anterior wrist ROI	Physical examination, GS (grey-scale) and PD (power Doppler) ultrasound; Tmean, Tmax, HDI (heat distribution index)	Moderate–severe arthritis vs. controls: Tmean ≥ 31.0 °C, AUC 0.93, sensitivity 85.7%, specificity 80%; Tmax ≥ 32.3 °C, AUC 0.91	Small subgroups; IRT less effective for mild arthritis	[40]
Cross-sectional study; 62 knee OA patients, 124 knees	Knee OA	FLIR E60 thermal camera (FLIR Systems, Inc., Wilsonville, OR, USA); 320 × 240 pixels; sensitivity < 0.05 °C; frontal/lateral/medial views; automated HSV (hue–saturation–value) segmentation	KL grade; mean and maximum skin temperature	Mean Tsk (skin temperature) increased with OA grade; grade 4 warmer than grades 2–3 in frontal/lateral views; age, BMI (body mass index), and disease duration affected Tsk	No US/MRI or biomarker comparator; no diagnostic accuracy analysis	[41]

Table 1. *Cont.*

Study Design/Population	Condition/Joint	Device/ Protocol	Comparator/ Thermal Metric	Statistical Thermographic Result	Main Limitation	Refs
Prospective cohort; 60 patients with joint pain	Mixed arthropathies/knee, ankle, elbow, wrist	FLIR T650sc thermal camera (FLIR Systems, Inc., Wilsonville, OR, USA); 640 × 480 pixels; sensitivity < 20 mK; standardized dark-room acquisition	Clinical exam plus ESR/CRP; mean temperature/intensity	IRT detected inflammation with sensitivity 91%, specificity 80%, PPV (positive predictive value) 94%, NPV (negative predictive value) 72%; detected 11/13 doubtful/subclinical cases	Heterogeneous joints and diseases; no US/MRI reference	[42]
Prospective imaging study; 20 children with JIA	JIA/knees	FLIR T630sc thermal camera (FLIR Systems, Inc., Wilsonville, OR, USA); 640 × 480 pixels; 20 s thermal video; anterior knee ROI tracking	Clinical musculoskeletal examination; ATD (absolute temperature difference), PTD (percentage temperature difference)	Active unilateral knees were warmer than inactive knees: median 31.30 vs. 30.33 °C; $p = 0.0078$; thermal and visual imaging agreed in 16/20 participants	Small sample; clinical exam rather than US/MRI reference	[43]
Case–control study; 30 RA patients, 22 controls	RA/fingers	FLIR E60bx thermal camera (FLIR Systems, Inc., Wilsonville, OR, USA); baseline, cold-water challenge, and 180 s rewarming; automated finger-axis analysis	RA vs. controls; Tmax–Tmin along each finger	Baseline temperatures were not significant; post-cooling Tmax–Tmin showed modest discrimination: AUC 0.61–0.68 for thumb–ring fingers	Modest AUC; no US/MRI comparator; dynamic thermoregulation may confound findings	[44]
Cross-sectional validation study; 56 knee OA patients	Knee OA/affected vs. contralateral knee	TOPDON TC001 thermal camera (Shenzhen TOPDON Technology Co., Ltd., Shenzhen, China); 256 × 192 pixels; 6 predefined knee ROIs	Contralateral knee, KL grade, WOMAC (Western Ontario and McMaster Universities Osteoarthritis Index), VAS (Visual Analogue Scale); mean ΔT	Affected knees were warmer: ΔT ≈ 1.8–2.0 °C, $p < 0.001$; ΔT correlated with KL grade, r = 0.442; cutoff 1.16 °C: sensitivity 95%, specificity 43%, AUC 0.65	Low specificity; no ultrasound/MRI/biomarker comparator	[16]
Prospective pediatric study; 40 rheumatic disease patients, 29 controls	Pediatric inflammatory arthritis/knee and ankle	FLIR ONE Edge Pro smartphone thermal camera (FLIR Systems, Inc., Wilsonville, OR, USA); 160 × 120 pixels; 20 min rest; 5 images per knee/ankle	Affected vs. unaffected joints; patients vs. controls; T-max, T-min, T-ave	Affected joints were warmer: knee T-max 34.25 vs. 32.70 °C, $p = 0.002$; ankle T-max 34.07 vs. 33.00 °C, $p = 0.011$; knee T-ave AUC 0.94, ankle T-ave AUC 0.91	Heterogeneous pediatric diseases; no US/MRI comparator	[45]
Cross-sectional study; 25 bilateral knee OA patients with unilateral symptoms	Knee OA/symptomatic vs. asymptomatic knee	FLIR E4 infrared camera (FLIR Systems, Inc., Wilsonville, OR, USA); anterior knee imaging; 15 min acclimatization	Contralateral knee, KL grade, VAS, pressure pain threshold; mean superficial temperature	No significant difference: symptomatic 31.2 ± 1.4 vs. asymptomatic 31.1 ± 1.5 °C, $p = 0.379$; no correlation with KL grade or pain	Small negative study; no synovitis imaging	[46]

Table 1. *Cont.*

Study Design/Population	Condition/Joint	Device/ Protocol	Comparator/ Thermal Metric	Statistical Thermographic Result	Main Limitation	Refs
Cross-sectional study; 70 RA patients	RA/right wrist	FLIR T640 thermal camera (FLIR Systems, Inc., Wilsonville, OR, USA); 640 × 480 pixels; sensitivity < 30 mK; 15 min acclimatization; dorsal wrist ROI	Clinical swelling/tenderness groups; US GS/PD; Tmax, Tavg, Tmin	Temperatures differed across wrist groups: Tmax $p = 0.002$, Tavg $p = 0.002$, Tmin $p = 0.008$; swollen wrists warmer than inactive wrists	Single wrist; cross-sectional; no MRI/structural damage comparator	[47]
Cross-sectional study; 81 RA patients, 810 MCP joints	RA/bilateral MCP 1–5	FLIR T865 thermal camera (FLIR Systems, Inc., Wilsonville, OR, USA); 640 × 480 pixels; sensitivity < 30 mK; dorsal MCP ROIs	US PD/GS; summed Tmax, Tavg, Tmin	Thermal sums correlated with PD more strongly than GS: PD r = 0.45–0.52, $p < 0.001$; AUC for PD ≥ 1 up to 0.82	MCP-only; no healthy control group	[48]
Cross-sectional study; 37 RA patients, 814 hand/wrist joints	RA/wrists, MCP, thumb IP, PIP	FLIR T640 thermal camera (FLIR Systems, Inc., Wilsonville, OR, USA); 640 × 480 pixels; sensitivity < 30 mK; dorsal hand/wrist ROIs	US PD/GS and clinical swelling/tenderness; Tmax, Tmin, Tavg, Tmax–Tmin	PD-positive joints were warmer: Tmax +1.37 °C, Tavg +1.16 °C, all $p < 0.001$; GS-positive joints also warmer, all $p < 0.001$	Small cohort; thermal findings did not clearly discriminate clinical swelling/tenderness categories	[49]
Cross-sectional multimodal study; 37 RA patients, 814 joints	RA/wrists, MCP, IP, PIP	FLIR T640 thermal camera (FLIR Systems, Inc., Wilsonville, OR, USA); adjusted joint temperatures; same-day US	DAS28; US PD/GS; MAX, MIN, AVG, and combined thermal–PD metrics	Thermography alone did not correlate with DAS28; combined thermal–PD metrics correlated with DAS28: MAX(PD) r = 0.393, $p = 0.016$	Small cohort; exploratory combined score; no external validation	[50]
Short clinical correspondence; 37 RA patients	RA/wrists, MCP, thumb IP, PIP	FLIR T640 thermal camera (FLIR Systems, Inc., Wilsonville, OR, USA); adjusted temperature and CTCA score	US PD/GS severity; clinical swelling/tenderness	Thermography alone predicted US inflammation at 3 sites; CTCA predicted inflammation at 6 sites; AUC 0.726–0.931	Short-format evidence; arbitrary CTCA weighting	[51]
Cross-sectional study; 95 RA (rheumatoid arthritis) patients, 190 knees	RA/bilateral knees	FLIR T640 thermal camera (FLIR Systems, Inc., Wilsonville, OR, USA); 640 × 480 pixels; sensitivity < 30 mK; 15 min acclimatization; lateral, anterior, and medial knee ROIs (regions of interest)	US (ultrasound) GS (grey-scale)/PD (power Doppler) synovitis at suprapatellar recesses; T-min, T-max, T-avg	Thermal parameters correlated with US inflammation: GS $\rho = 0.27–0.49$, $p < 0.01$; PD $\rho = 0.21–0.43$, $p < 0.05$. ROC AUCs (receiver operating characteristic area under the curve) reached 0.82 for PD positivity and GS ≥ 2; intra-observer reliability ICC (intraclass correlation coefficient) 0.997–0.999	Cross-sectional; no healthy controls; US limited to suprapatellar recess; no longitudinal/treatment-response data	[52]

Table 1. *Cont.*

Study Design/Population	Condition/Joint	Device/ Protocol	Comparator/ Thermal Metric	Statistical Thermographic Result	Main Limitation	Refs
Cross-sectional study; 42 RA patients, 420 clinically quiescent MCP joints	RA/subclinical MCP inflammation	FLIR T640 thermal camera (FLIR Systems, Inc., Wilsonville, OR, USA); dorsal MCP ROIs; summed temperatures	US GS/PD; Total Tmin, Total Tavg, Total Tmax	Thermal sums correlated with subclinical US inflammation: GS r = 0.421–0.430; PD r = 0.383–0.424	MCP-only; no healthy control group	[53]
Cross-sectional study; 87 RA patients	RA/right wrist	FLIR T640 thermal camera (FLIR Systems, Inc., Wilsonville, OR, USA); wrist ROI	Clinical wrist status; US GS/PD; Tavg, Tmax, Tmin	Symptomatic wrists warmer than asymptomatic; asymptomatic wrists with US synovitis warmer than those without, p = 0.007–0.008	Single wrist; no longitudinal follow-up	[54]
Brief cross-sectional study; 30 RA patients, 60 elbows	RA/bilateral elbows	FLIR T640 thermal camera (FLIR Systems, Inc., Wilsonville, OR, USA); anterior/posterior/medial/lateral elbow views	US GS/PD; summed MIN, MAX, AVG	Thermal metrics correlated with PD bilaterally: right r = 0.40–0.47, left r = 0.45–0.55; GS correlation inconsistent	Small sample; no healthy or disease-control group	[55]
Cross-sectional study; 80 early RA patients, 2080 joints by US	RA/clinically quiescent wrists and MCPs	FLIR T640 thermal camera (FLIR Systems, Inc., Wilsonville, OR, USA); hand/wrist ROIs at frequent subclinical PD sites	26-joint US PD; DAS28 groups; Total Tmax, Tavg, Tmin	Higher temperatures when TPD > 1: Total Tmax p = 0.007, Tavg p = 0.013, Tmin p = 0.019; AUC 0.789–0.810	Selected thermography sites; no longitudinal validation	[56]
Multicenter case–control study; 151 knee OA patients, 157 controls	Knee OA/lower-limb acupoints	TMI-M portable medical infrared thermal imager (Beijing Wholelife Medical Science Co., Ltd., Beijing, China); 256 × 336 pixels; 11 acupoints	Non-knee OA controls; relative/absolute STA	Relative STA higher in KOA at ST34, EX-LE2, EX-LE5, SP10, BL40, and GB39, $p \leq 0.0037$; four thermal clusters higher, $p < 0.01$	Acupoint-focused; no US/MRI or synovitis comparator	[57]
Cross-sectional case–control study; 52 RA patients, 26 controls	RA/bilateral MCP and PIP joints 1–5	FLIR T450sc thermal camera (FLIR Systems, Inc., Wilsonville, OR, USA); 320 × 240 pixels; 20 MCP/PIP ROIs	Healthy controls; RAI; mean joint temperature	RA joints warmer than controls, $p < 0.05$; temperature increased with RAI score: 32.43 °C at RAI 0 to 33.60 °C at RAI 3	No US/MRI comparator; acquisition conditions incompletely reported	[58]
Pilot case–control study; 50 RA patients, 50 controls	RA/knee	Testo 885 infrared camera (Testo SE & Co. KGaA, Titisee-Neustadt, Germany); 320 × 240 pixels; lateral knee and mid-thigh AOIs	Healthy controls; PDUS grade 0–3; knee–thigh ΔT	RA knees warmer: 32.732 vs. 31.490 °C; knee–thigh ΔT +1.080 vs. −0.516 °C; AUC 99.8%, cutoff 0.15 °C, sensitivity 100%, specificity 94.35%	Pilot study; healthy controls; PDUS-grade separation not significant	[59]

Table 1. *Cont.*

Study Design/Population	Condition/Joint	Device/ Protocol	Comparator/ Thermal Metric	Statistical Thermographic Result	Main Limitation	Refs
Development + validation study; 51 JIA patients, 48 controls, 43 validation patients	JIA/knees and ankles	FLUKE TiR32 thermal imager (Fluke Corporation, Everett, WA, USA); 320 × 240 pixels; sensitivity ≤ 0.04 °C; standardized lower-limb views	Development: US; validation: rheumatologist exam; TAWiC mean/95th percentile	TAWiC improved performance vs. absolute temperature: 95th anterior TAWiC AUC 0.867 vs. absolute 0.659; validation sensitivity 0.60–0.70, specificity > 0.90	Small validation cohort; ankle validation limited; posterior knee view weak	[60]

Table 2. Computational and machine-learning thermography studies.

Study Design/ Dataset	Condition/Joint	Device/ Protocol	Computational Method	Comparator/ Validation Reference	Model Performance Result	Main Limitation	Refs
Computational diagnostic study; 100 participants: 50 RA (rheumatoid arthritis) patients and 50 healthy controls; 600 hand thermograms augmented to 1440 training images	RA/hand thermal images	FLIR A305SC thermal camera (FLIR Systems, Inc., Wilsonville, OR, USA); controlled room at 20 °C; 15 min acclimatization; 1 m distance; dorsal, ventral, and AP (anteroposterior) views of both hands	Custom RANet CNN (convolutional neural network), pretrained CNNs, QNN (quanvolutional neural network), and RANet feature extraction with ML (machine learning) classifiers	Rheumatologist-confirmed RA vs. healthy controls; 80/20 train-test split and 70/30 train-validation split	RANet accuracy 95%; RANet + SVM (support vector machine) accuracy 97%; QNN accuracy 93.33%, precision 0.96, recall 0.92, F1-score 0.93	Limited real dataset; heavy augmentation; no external validation	[61]
Computational classification study; 60 participants: 30 RA patients and 30 healthy controls; 240 hand thermograms	RA/bilateral hand thermal images, dorsal and ventral views	FLIR A305SC thermal camera (FLIR Systems, Inc., Wilsonville, OR, USA); 15 min acclimatization; dark room at 20 °C; humidity 45–50%; 1 m distance; fixed scale 25.5–35.5 °C	Color-based k-means segmentation of hot spots; BRISK (Binary Robust Invariant Scalable Keypoints), MSER (Maximally Stable Extremal Regions), FAST (Features from Accelerated Segment Test), Harris, ORB (Oriented FAST and Rotated BRIEF), feature fusion, classical ML classifiers, and QSVM (quantum support vector machine)	Rheumatologist-confirmed RA vs. healthy controls; 10-fold cross-validation and 80/20 train-test split	RA hands had higher temperatures at PIP (proximal interphalangeal), MCP (metacarpophalangeal), and palm ROIs (regions of interest), $p \leq 0.03$; LogitBoost accuracy 93.75%, AUC (area under the curve) 0.99; QSVM accuracy 92.7%, F1-score 0.94	Limited dataset; handcrafted feature extraction; no external validation	[62]

Table 2. *Cont.*

Study Design/ Dataset	Condition/Joint	Device/ Protocol	Computational Method	Comparator/ Validation Reference	Model Performance Result	Main Limitation	Refs
Technical/computational classification study; 110 knee thermograms: 60 arthritis and 50 non-arthritis/healthy or knee-pain thermograms; arthritis group included 20 RA, 20 OA (osteoarthritis), and 20 reactive arthritis thermograms	Knee arthritis/RA prediction from knee thermograms	FLIR T650sc thermal camera (FLIR Systems, Inc., Wilsonville, OR, USA); 640 × 480 pixels; sensitivity 0.02 °C at 30 °C; room 22 °C; 15 min acclimatization; anterior knee view within 2 m	Modified multi-seeded region-growing segmentation; shape, texture, and frequency features; SVM classifier; SVM-RFE (support vector machine–recursive feature elimination), RELIEF, and accuracy-based feature selection	Expert ground-truth inflammation masks; arthritis vs. non-arthritis and RA vs. non-RA arthritis; threefold cross-validation	Segmentation accuracy 98.6%; first-stage arthritis classification accuracy 91%, sensitivity 0.93, specificity 0.90; second-stage RA classification accuracy 73%, AUC 0.72	Small dataset; only 20 RA thermograms; modest RA classification performance; no external validation	[63]
Technical segmentation study; 50 arthritis knee thermograms and 44 abnormal breast thermograms	Knee arthritis/knee thermograms	Gray-palette knee thermograms acquired under standardized medical supervision; camera model/manufacturer not clearly reported	RASIT (region-shrinking segmentation based on image temperature); electrostatic-force image computation, automatic weighted thresholding, iterative ROI extraction	Expert-validated ground-truth masks; compared with Otsu, Kapur, PSO (particle swarm optimization), k-means, FCM (fuzzy c-means), EM (expectation–maximization), region growing, FODPSO, and MTEMO	For knee thermograms: DSC (Dice similarity coefficient) 0.805, accuracy 98.2%, sensitivity 0.857; significant differences vs. most methods, $p < 10^{-6}$	Segmentation only; small knee dataset; manual cropping; device details incomplete	[64]
Diagnostic ML study; 100 participants: 70 RA patients and 30 healthy controls	RA/MCP and PIP joints of both hands	FLIR T450sc infrared camera (FLIR Systems, Inc., Wilsonville, OR, USA); 320 × 240 pixels; NETD (noise-equivalent temperature difference) < 30 mK; emissivity 0.98; 24 °C room; 15 min acclimatization; static and alcohol-cooling dynamic thermography	Snake algorithm for background removal; skeletonization for MCP/PIP localization; SIFT (scale-invariant feature transform) + RANSAC (random sample consensus) alignment; SVM, KNN (k-nearest neighbors), and decision-tree classifiers; 5-fold cross-validation	Clinical RA vs. healthy controls; RAI (Ritchie Articular Index) mapped to MCP/PIP joints	Dynamic parameters differed across RAI levels for Tcooling, $p = 0.025$, and Trewarming, $p = 0.042$; static-temperature SVM accuracy 93%, precision 92.9%, recall 97%, F1-score 95%	Single-center dataset; class imbalance; no external validation; cooling protocol may be operator-dependent	[65]

Table 2. *Cont.*

Study Design/ Dataset	Condition/Joint	Device/ Protocol	Computational Method	Comparator/ Validation Reference	Model Performance Result	Main Limitation	Refs
Technical segmentation study; 50 inflammatory knee-joint thermograms plus breast thermography datasets	Inflammatory knee joint disease/knee thermograms	FLIR T650sc thermal camera (FLIR Systems, Inc., Wilsonville, OR, USA); 640 × 480 pixels; sensitivity < 20 mK; 15 min stabilization; camera 2 m from patient	Extended region-growing segmentation with logarithmic transformation, automatic multi-seed selection, modified similarity/stopping criteria, and intersection of original/filtered segmentations	Clinically validated ground-truth masks; compared with FCM, k-means, region growing, Otsu, mean-shift, and FODPSO	Knee thermograms: Jaccard index 0.68, Dice similarity 0.79, recall 0.81, precision 0.83, accuracy 98.07%; Kruskal–Wallis testing favored proposed method, $p < 0.05$	Segmentation only; relatively small knee dataset; no diagnostic classifier or external clinical validation	[66]
Technical segmentation study; 100 arthritic knee thermograms from a 200-image inflammatory knee thermogram dataset	Arthritis/knee thermograms	Existing inflammatory knee thermogram dataset; acquisition device/manufacturer not specified	Cluster-ensemble segmentation using AMSS (anisotropic mean shift smoothing) edge enhancement, FCM clustering, VOI (volume/region of interest)-based consensus, and Greedy ICM (iterated conditional modes) refinement	Ground-truth segmentation masks; compared with k-means, FCM, region growing, RASIT, LSNAP, COIK-means, and DSIMFc	Precision 0.7324, recall 0.9197, accuracy 0.9800, over-segmentation 0.0784, under-segmentation 0.2824	Preprint; segmentation only; no diagnostic validation; device details not reported	[67]
Computational classification study using the public Infrared Knee Joint Dataset; subset of posterior-view knee thermograms from healthy, RA, and OA groups	Arthritis/knee thermograms	FLIR T650sc thermal camera (FLIR Systems, Inc., Wilsonville, OR, USA); 640 × 480 pixels; sensitivity 0.02 °C; posterior knee view at 2 m	Modified k-means segmentation of HA (hyaluronic acid)-related regions; connected-component analysis; CHA (computed hyaluronic acid proxy) feature; handcrafted features + ML classifiers; VGG19 + CHA comparison	Dataset labels: healthy, RA, OA; compared with prior SVM and VGG19 methods	CHA differed between groups; best conventional ML: Naive Bayes accuracy 96.38%; VGG19 + CHA accuracy 97.22%	CHA is image-derived, not biochemically measured; posterior view only; no external validation	[68]
Multimodal computational classification study; 100 participants: 50 RA patients and 50 controls; 200 radiographs and 200 thermal images	RA/hands, PIP and MCP regions	FLIR A305SC thermal camera (FLIR Systems, Inc., Wilsonville, OR, USA); thermal images acquired in a 20 °C dark room at 1 m; AP hand radiographs also acquired	Thermal hot-spot segmentation with color-based k-means; SURF (Speeded-Up Robust Features); ML classifiers; fine-tuned CNNs; custom RA-XTNet CNN; ViT (vision transformer); QSVM	Rheumatologist-confirmed RA vs. controls; train/test validation	Thermal imaging outperformed radiographs; RA-XTNet thermal accuracy 92.5%, AUC 0.96; QSVM thermal accuracy 93.75%, precision 0.88, recall 1.00, F1-score 0.93	Small single-center dataset; established RA mainly; no external validation	[69]

Table 2. *Cont.*

Study Design/ Dataset	Condition/Joint	Device/ Protocol	Computational Method	Comparator/ Validation Reference	Model Performance Result	Main Limitation	Refs
Dual-center computational regression study; Xinhua dataset: 93 knee-disease patients and 2 controls; Meinian dataset: 24 KOA (knee osteoarthritis) patients and 19 controls	KOA/knee pain prediction	Front-view lower-body thermal images; thermal-camera models/manufacturers not clearly specified; combined with age, sex, height, weight, BMI (body mass index), disease duration, and VAS (Visual Analogue Scale) pain score	Background removal, knee ROI extraction, grayscale thermal features: AGV (average gray value), MGV (maximum gray value), APGV (average positive gray value), temperature; regression models including ElasticNet, SVR (support vector regression), random forest, and XGBoost	VAS pain prediction; KL (Kellgren–Lawrence) grade correlation; single-center, cross-center, and mixed dual-center validation	VAS and KL grade had almost no linear correlation, r = −0.00413; best model: XGBoost mixed dual-center split, MSE (mean squared error) 1.4634, R^2 0.7649, MAE (mean absolute error) 0.9094	Predicts subjective pain, not inflammation/OA diagnosis; camera details incomplete; small datasets	[70]
Cross-sectional ML validation study; 595 participants; development set 449 mixed hand conditions/controls; validation set 146 RA patients	RA/hands, wrists, MCP and PIP joints	Smartphone-connected FLIR One Pro (FLIR Systems, Inc., Wilsonville, OR, USA) or Thermal Expert TE-Q1 (i3system Inc., Daejeon, Republic of Korea); real-world dorsal hand imaging without acclimatization or controlled temperature	Automated preprocessing, noise reduction, background removal, contrast enhancement, ROI/feature extraction; KNN algorithm generated ThermoJIS (thermographic joint inflammation score)	US GS/PD synovitis across wrists, MCP 1–5, and PIP 1–5 bilaterally	ThermoJIS correlated with US GS sum score, ρ = 0.49, $p < 0.001$, and PD sum score, ρ = 0.51, $p < 0.001$; active synovitis AUROC 0.78; cutoff 3.56: sensitivity 94%, specificity 51%, NPV 88%	Internal validation only; tenosynovitis not assessed; real-world acquisition may reduce reproducibility	[71]
Short-report validation study; 146 RA patients from ThermoJIS validation cohort	RA/hands, wrists, MCP and PIP joints	Thermal Expert TE-Q1 smartphone-connected camera (i3system Inc., Daejeon, Republic of Korea); dorsal hand thermograms; real-world acquisition without acclimatization	ThermoJIS plus PGA (patient global assessment) to form ThermoDAI (thermographic disease activity index); ThermoJIS + PGA + CRP to form ThermoDAI-CRP	US GS/PD synovitis; CDAI (Clinical Disease Activity Index), SDAI (Simplified Disease Activity Index), DAS28-CRP (Disease Activity Score in 28 joints using C-reactive protein)	ThermoDAI-CRP correlated with US GS ρ = 0.58 and PD ρ = 0.61, both $p < 0.001$; correlated with SDAI ρ = 0.85 and DAS28-CRP ρ = 0.81, both $p < 0.001$	Cross-sectional; same cohort as ThermoJIS validation; low specificity for remission-threshold detection	[72]

Table 2. *Cont.*

Study Design/ Dataset	Condition/Joint	Device/ Protocol	Computational Method	Comparator/ Validation Reference	Model Performance Result	Main Limitation	Refs
Prospective longitudinal external-validation study; 77 RA patients from 3 hospitals; 73 completed 12-week follow-up	RA/hands; disease activity and swollen-joint assessment	Thermal Expert TE-Q1 smartphone-connected camera (i3system Inc., Daejeon, Republic of Korea); dorsal hand thermograms; real-world outpatient acquisition without acclimatization	Pretrained ML model generated ThermoJIS; ThermoDAI and ThermoDAI-CRP calculated	Clinical indices: SJC28 (swollen joint count in 28 joints), TJC28 (tender joint count in 28 joints), PGA, EGA (evaluator global assessment), CDAI, SDAI, DAS28-CRP; ACR (American College of Rheumatology) and EULAR (European Alliance of Associations for Rheumatology) response	ThermoJIS detected SJC28 > 1 with AUROC 0.67; ThermoDAI correlated with CDAI, $\rho = 0.81$; ThermoDAI-CRP correlated with SDAI, $\rho = 0.83$; ThermoDAI-CRP detected ACR20 with AUROC 0.80 and ACR50 with AUROC 0.91	No US reference in external validation; modest sample; 12-week follow-up only	[73]
Computational diagnostic study; 65 RA patients and 104 healthy controls	RA/fingers of both hands	FLIR E60bx thermal camera (FLIR Systems, Inc., Wilsonville, OR, USA); 320 × 240 pixels; dynamic cooling in 0 °C water for 5 s followed by 180 s rewarming	Univariate logistic regression for predictor selection; feedforward ANN (artificial neural network); 75/25 train-test split; 10-fold cross-validation; BFGS (Broyden–Fletcher–Goldfarb–Shanno) training	RA vs. healthy status; clinical/laboratory variables including BMI, ESR, CRP, WBC (white blood cell count), and thermal recovery metrics	ΔTr (temperature recovery difference) was lower in RA for all fingers, $p < 0.05$; ANN sensitivity 81.25%, specificity 100%, accuracy 92.86%, Kappa 0.72	Model combines thermography and lab variables; independent value of IRT unclear; no external validation	[74]
Computational diagnostic study; 477 hand thermograms: 291 controls and 186 RA images; strict patient-level train/test split	RA/dorsal hand thermograms after cold provocation	FLIR E60bx thermal camera (FLIR Systems, Inc., Wilsonville, OR, USA); 320 × 240 pixels; sensitivity < 0.045 °C; 15 min acclimatization; 0 °C cooling for 5 s; 180 s rewarming; frames at 60, 120, 180 s	SNNs (spiking neural networks) with static-to-dynamic spike encoding; Tempotron, SGL (surrogate gradient learning), and BAL (bio-inspired active learning); preprocessing with segmentation and skeletonization	RA vs. healthy-control classification; strict patient-level validation and GroupKFold cross-validation	Best fixed split: Tempotron accuracy 90.62%, ROC AUC 0.9153, macro F1-score 0.8982; GroupKFold mean ROC AUC 0.82–0.84	Single-center dataset; no external validation; classifies RA vs. healthy, not synovitis severity	[75]

Table 2. *Cont.*

Study Design/ Dataset	Condition/Joint	Device/ Protocol	Computational Method	Comparator/ Validation Reference	Model Performance Result	Main Limitation	Refs
Computer-assisted imaging study; 60 participants: 30 RA patients and 30 controls	RA/knee region	Knee radiographs plus bilateral knee thermograms; FLIR thermal camera, model/manufacturer not specified; 15 min acclimatization; 1 m distance	X-ray segmentation with fast greedy snake algorithm; thermal RGB (red-green-blue)-based binary-mask segmentation; GLCM (gray-level co-occurrence matrix) and statistical feature extraction	RA vs. controls; ESR, CRP, DAS (disease activity score), HAQ	Thermal skin temperature correlated with ESR r = 0.758, CRP r = 0.739, DAS r = 0.735, HAQ r = 0.519; $p < 0.05$–0.01	No diagnostic classifier or external validation; camera model incompletely reported	[76]
Clinical image-processing study; 60 participants: 30 RA patients and 30 controls	RA/knee region	FLIR ThermaCAM T400 thermal camera (FLIR, Täby, Sweden); NETD < 50 mK; 10 min acclimatization; standing and sitting/flexed knee thermograms; CDUS (colour Doppler ultrasound) also performed	RIBS (regional isotherm-based segmentation), Otsu thresholding, HSV (hue–saturation–value) conversion, hot-spot detection, connected-component analysis, GLCM/statistical features; ImageJ CDUS segmentation	RA vs. controls; CDUS effusion/perfusion/color fraction; ESR, CRP, DAS, HAQ	RA knees warmer: 33.99 ± 0.9 vs. 31.97 ± 0.7 °C, $p = 0.03$; thermal temperature correlated with HAQ r = 0.75, DAS r = 0.70, ESR r = 0.75, CRP r = 0.64; all $p < 0.01$	Small sample; no independent validation; no diagnostic accuracy metrics for CAD model	[77]
Computer-aided diagnostic image-analysis study; 60 participants: 30 RA patients and 30 controls	RA/hand MCP and PIP joints	FLIR ThermaCAM T400 thermal camera (FLIR, Täby, Sweden); 320 × 420 thermal detector; NETD < 50 mK; 10 min acclimatization; AP and PA (posteroanterior) hand thermograms; 18 joints per subject	k-means and FCM segmentation after RGB-to-HSV conversion; statistical and GLCM feature extraction; CAD (computer-aided diagnosis) interface; ROC analysis for MCP classification	RA vs. healthy controls; Indian Rheumatology Association RA criteria	MCP2 and MCP3 were warmer in RA: MCP2 35.40 ± 0.6 vs. 33.66 ± 0.2 °C, $p = 0.003$; MCP3 35.52 ± 0.7 vs. 33.74 ± 0.2 °C, $p = 0.001$; ROC sensitivity 86.6%, specificity 79%; k-means outperformed FCM	Small sample; no US/MRI comparator; no external validation; RA vs. healthy only	[78]

3.1. Pathophysiological Basis of Thermal Changes in Arthropathies

Rheumatoid arthritis (RA) illustrates this inflammation–temperature relationship. Chronic synovitis causes hyperemia and increased metabolic activity, resulting in higher skin temperature in the affected area [49]. Preliminary infrared studies have shown that inflamed rheumatoid arthritis joints produce more heat than non-inflamed joints [49]. Any active form of arthritis can display a detectable heat signature; therefore, this is not exclusive to rheumatoid arthritis. For example, even in cases of "degenerative" arthropathy, there is low-grade synovial inflammation. The knee affected by osteoarthritis (OA) is often 1–2 °C warmer than the opposite, healthy knee [16]. Charcot neuroarthropathy, sometimes called neuropathic osteoarthropathy, causes the most significant temperature changes. In advanced stages of Charcot, the affected foot may have a temperature increase of more than 2 °C compared to the unaffected side [32], with reported differences ranging from 3 °C up to 4.6 °C in most severe cases [79,80]. A key clinical sign of active Charcot is a foot temperature difference; in this case, the disparity between the two sides is so pronounced that strict climate-controlled imaging may not be necessary [32]. This suggests that, besides inflammation, the main factors affecting temperature fluctuations in arthropathies are enhanced blood flow and resulting edema.

However, these temperature patterns can be influenced by disease-specific vascular issues. In psoriatic arthritis (PsA), inflamed entheses and joints cause significant cutaneous vasodilation; yet, microvascular damage in chronic rheumatoid arthritis (RA) may unexpectedly reduce heat emission in some individuals. Unlike findings in PsA, a functional thermal imaging study showed that RA patients had lower skin temperatures in their hands compared to healthy controls after activity [30]. The authors proposed that chronic inflammation and vasculopathy impair normal thermoregulatory responses, whereas PsA joints either preserve or increase heat under stress [30]. Despite these differences, the fundamental link between heat and inflammation remains. A hot-spot on thermography, indicating synovitis, is seen in most inflamed joints of individuals with active RA or PsA [49,81]. Localized heat may also occur in osteoarthritic joints during inflammatory events like effusion or synovitis flare-ups [82]. Using modern infrared tools to detect and measure these thermal signals can improve our understanding of how the disease affects the body, as discussed further in the following sections.

3.2. Technical Principles of Infrared Thermography

Infrared (IR) thermography is a non-invasive imaging technology that assesses the body's temperature by detecting long-wave IR radiation emitted from the skin and turns it into temperature maps (Figure 2) [17]. Acclimating the patient in a controlled environment (draft-free room, approximately 22 °C) for around 15 min to stabilize skin temperature is a standard approach in musculoskeletal applications [51]. The camera is positioned perpendicular to the area of interest and maintained at a fixed distance (about 50–100 cm for knees and hands) with a skin emissivity calibration of roughly 0.98 [51]. Patients are required to remove any jewelry or clothing that may cover the area and maintain a consistent posture (e.g., hands flat on a table for hand imaging) to enable uniform positioning and picture acquisition [51,83]. To prevent the introduction of artifacts into the data, it is essential to stick to specific rules while detecting temperature differentials.

Basic spot measurements at designated locations (e.g., handheld infrared thermometers) were extensively utilized in initial thermographic investigations. Infrared "dermal thermometers" have remarkable inter-rater reliability [32] when used to assess single-point temperatures, namely at the instep and arch of the foot in Charcot arthropathy. Dallimore et al. demonstrated substantial intra- and inter-observer concordance (intraclass correlation values between 0.87 and 0.99 interpreted as good-to-excellent) across 10 anatomical

foot sites by testing a methodology using both tactile and non-contact portable infrared devices on Charcot feet [32]. They found that a "scanning" technique, which did not require the probe to contact the skin, was equally reliable, demonstrating that contemporary equipment can accurately obtain readings without direct contact [32]. Recent studies use comprehensive thermographic cameras to capture images of the entire joint rather than a singular location. The software subsequently extracts characteristics including maximum (T_max), minimum (T_min), and average (T_avg) temperatures within each region of interest (ROI), which may be detected manually or automatically [49,51]. In quantitative thermography for arthritis, these factors are of paramount importance because they allow objective comparison between affected and healthy joints, monitoring of pathological activity, and ensure differences between inflammatory and non-inflammatory states [84,85]. In RA hand imaging, it is standard procedure to delineate ROIs encompassing all joints (wrist, MCP, and PIP joints) and document the maximum, minimum, and average temperatures at each joint [51]. Thermographic indices can also be obtained by measuring a temperature and subtracting a reference temperature, such as the coldest joint or adjacent skin, to adjust for fluctuations in body temperature [51]. Tan et al. employed this procedure to tackle the problem of inter-patient baseline variability. They accomplished this by deducting the minimum finger temperature from each joint's measurement, which allowed a more accurate identification of the inflammatory sites [51]. A metric referred to as TAWiC (Temperature After Within-limb Calibration) is used in pediatric arthritis research to assess joint temperature in the same limb, excluding the mid-shaft skin temperature, to account for overall limb warmth [86]. These calibration approaches boost sensitivity by removing any confounding factors, like fluctuations in external temperature or systemic blood flow.

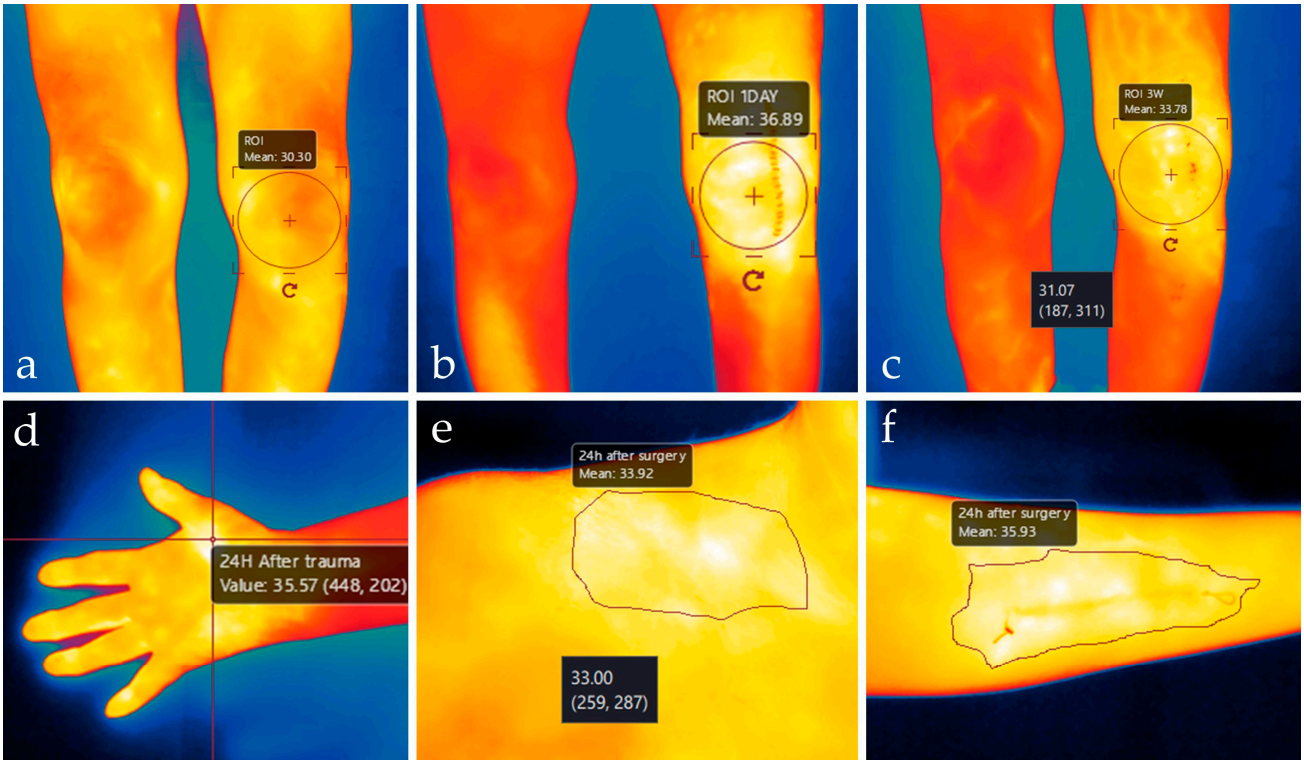

Figure 2. Representative infrared thermographic images illustrating regional temperature variations in joint, post-traumatic, and postoperative settings. (**a**–**c**) Serial thermographic assessment of the knee joint demonstrating increased local temperature at baseline (**a**), peak inflammatory activity at 1 day ((**b**); ROI mean: 36.89 °C), and partial resolution at 3 weeks ((**c**); ROI mean: 33.78 °C); (**d**) Thermographic image of the hand 24 h after trauma, showing focal hyperthermia (mean: 35.57 °C) corresponding to the injured region; (**e**) Thermographic assessment of the shoulder region following

clavicular fracture fixation, demonstrating diffuse temperature elevation over the deltoid and periarticular areas (ROI mean: 33.92 °C); and (**f**) Postoperative thermographic image of the arm at 24 h, showing heterogeneous thermal distribution (ROI mean: 35.93 °C), reflecting regional differences in perfusion and early healing response. The thermographic images are original and were acquired by the authors at "Foișor" Clinical Hospital of Orthopaedics, Traumatology and Osteoarticular TB.

Thermal imaging has evolved from a solely visual medium to one that employs intricate computational analysis. Automated segmentation methods are effective for the objective isolation of joints. Umapathy et al. [77] conducted a study employing automated analysis of Doppler ultrasound images alongside a regional isotherm-based segmentation (RIBS) technique to segment knee thermal images. Another study effectively differentiated rheumatoid arthritis from healthy patterns through deriving statistical characteristics (mean, variance, and entropy of heat distribution) from knee images utilizing a computer-aided diagnostic method [76]. Recently, thermographic data has been directly utilized in machine learning and deep learning (more details are provided in Section 3.5). An analysis successfully detected rheumatoid arthritis from hand thermographs using a proprietary convolutional neural network ("RANet") without human interaction in ROI selection [61]. Another innovative approach combined biomechanics with autonomous tracking of dynamic knee regions, utilizing a DeepLabCut model, a deep learning instrument for posture estimation [17]. Using sensor fusion, the team accurately measured the knee's surface temperature during exercise without markers, providing functional results that surpassed static images [17].

Stringent standardization is a recurring theme in the literature. Minor alterations in approach can result in considerable variations in temperature readings. Researchers often control the humidity and temperature of the environment, employ a standardized camera with consistent parameters (including distance and angle), and allow patients to acclimatize prior to the commencement of the study [51]. For instance, Sharma et al. achieved a test–retest correlation coefficient of r = 0.985 for knee thermal measurements under regulated conditions [16], indicating exceptional test–retest reliability when protocols are precisely adhered to. Conversely, a major barrier to medical adoption and comparative studies is the lack of standardization [16]. Another technical point is resolution: the small joints of the hands and feet require high spatial resolution to differentiate individual joints. Modern cameras (e.g., 640 × 480 pixels with <30 mK sensitivity) are generally adequate [17,51], but older or lower-spec devices might miss subtle changes. Finally, one can perform dynamic thermography by applying stimuli, such as a cold challenge or exercise, to probe vascular reactivity. RA vs. healthy discrimination has been achieved by observing rewarming curves of fingers after cold stress [44], and as noted, exercise-induced thermal responses differentiate disease states in RA/PsA [30].

3.3. Thermographic Patterns Across Arthropathies

Thermography has disclosed both prevalent patterns and unique characteristics in several joint disorders. Focal hotspots on thermal imaging consistently indicate actively inflammatory joints, irrespective of the underlying disease. In rheumatoid arthritis (RA), multiple studies have shown that synovitis-positive joints consistently have elevated temperatures relative to non-synovitis-positive joints. Tan et al. [49] discovered that clinically quiescent joints exhibited temperatures around 1.1–1.4 °C lower than rheumatoid arthritis finger and wrist joints with a power Doppler signal. Similarly, joints displaying grey-scale synovial hypertrophy showed skin temperatures approximately 1 °C higher than those without ultrasonic inflammation [49]. These differences were highly significant and illustrate a reproducible RA pattern: inflamed joints (whether tender or not) tend to radiate more heat. Morales et al. likewise reported that their Thermographic Joint Inflammation

Score (aggregating hand joint temperatures) was significantly higher in RA patients with ultrasound-confirmed synovitis—even in patients who were in clinical remission by exam criteria [71]. Rheumatoid arthritis causes affected joints to have detectable thermal readings, which frequently correspond with inflammation not apparent during a clinical examination.

In osteoarthritis, the increase in temperature in affected joints is less pronounced, but it remains evident. In knee OA, a common symptom is the asymmetry between the affected and unaffected knees. Sharma et al. [16] found that, on average, osteoarthritic knees exhibited a temperature increase of 1.8 °C compared to the contralateral knees. The temperature asymmetry distinctly influences one knee, and this effect remained consistent across the sample (effect size d = 2.81) [16]. A high value of the effect size, as mentioned in the study of Sharma et al. is exceptionally large for a skin-temperature endpoint, thus it should be interpreted with caution, because it could reflect highly controlled acquisition conditions, selected sample characteristics, and the use of a non-OA knee as comparator, rather than a generalizable population-level effect. Other replication studies in less selected cohorts should be further performed under routine clinical conditions to treat this value as representative. A strong correlation exists between disease severity and the extent of temperature elevation in osteoarthritis (OA). Moderate relationships exist between temperature shifts and Kellgren–Lawrence radiography grades [16]. The spatial distribution of knee OA thermograms may indicate inflammation. A greater temperature along the medial joint line may indicate synovitis or irritation of an osteophyte. Osteoarthritis patterns are typically less severe than rheumatoid arthritis patterns. An increase of one to two degrees is typical, although rheumatoid joints exhibiting active synovitis may frequently have elevations above one degree.

Enthesitis and dactylitis can alter the pathophysiology of spondyloarthritides such as PsA. Thermography in PsA can reveal inflamed tendon insertions or significant warmth in a digit (termed a “sausage digit”) [87], in contrast to the joint-centered hot spots observed in RA. Capo et al.’s study contrasting PsA and RA revealed that the two disorders are distinct: an earlier investigation showed that PsA patients exhibited markedly greater post-exercise temperature fluctuations in specific hand regions compared to healthy controls; however, a later study involving RA patients did not reproduce this finding [30]. In contrast, the initial hand temperatures of RA patients were somewhat lower than those of the control group, showing a diminished microvascular response [30]. It can be inferred that, despite both RA and PsA being inflammatory conditions, the thermographic patterns they produce may vary. For example, PsA may demonstrate increased hyperthermia abruptly in inflamed areas, whereas RA may intermittently show cooler regions, indicating chronic microvessel injury. Increased core body temperatures in afflicted joints are a characteristic hallmark of active rheumatoid arthritis, characterized by severe inflammation. A “cool” rheumatoid arthritis joint with thermography may indicate remission or persistent alterations in blood flow, rather than contradicting the inflammation-heat paradigm.

Peripheral arthropathies linked to neuropathy or diabetes show considerable sensations of heat. For example, the foot becomes significantly heated during the acute phase of diabetic Charcot arthropathy [88]. Physicians may clearly observe the swollen foot in comparison to a normal foot. The foot thermogram may display a consistent increase in temperature in the midfoot and hindfoot regions. A disparity of 2 °C across feet is deemed serious, and sequential infrared thermometer evaluations are already a common intervention for Charcot feet. Thermography quantitatively validates this trend. A reliability study indicated that the Charcot side of the foot consistently presented a temperature elevation of several degrees compared to the contralateral side across ten frequent regions (forefoot, midfoot, heel, etc.) [32]. Prior to declaring this pattern resolved, the acute inflammation must be addressed. Charcot’s thermal signature is characterized by extensive inflammatory

osteolysis, appearing as generalized warmth in the foot. This differs from RA, which triggers localized hot patches in the joints. Osteomyelitis of the foot may induce fever, complicating the differentiation between an infection and Charcot arthropathy alone through thermography. Nonetheless, both conditions exhibit the identical "hot foot" pattern.

A critical distinction in pattern interpretation is that thermography has not been shown to be consistently beneficial for all joints in all studies. Jones et al. discovered that hand thermography failed to distinguish between those with active rheumatoid arthritis, as determined by clinical or laboratory criteria, and those without [39]. Thermal imaging may fail to identify moderate inflammation in small joints, as no correlation was found between average hand joint temperatures, swollen joint counts, or C-reactive protein levels in that cohort [39]. The "pattern" of heat in rheumatoid arthritis is evident at the individual joint level with moderate-to-severe synovitis; however, quantifying mild or diffuse warmth in numerous tiny joints can be challenging. This singular negative outcome should be viewed as a warning. The study averaged focus signals across joints using an earlier FLIR T300 camera (FLIR Systems, Inc., Wilsonville, OR, USA), possibly diminishing their clarity. So, outdated technology may have also been a contributing factor [39].

Thermography has been used to differentiate between normal healing and disease in postoperative joints, as well as in instances of inflammatory arthritides. Post-total knee arthroplasty (TKA), transient warmth is a frequent sensation, typically subsiding shortly thereafter. A convincing study by Windisch et al. revealed that daily monitoring of skin temperature around the knee post-TKA showed minimal variation over the surgical incision, while the less affected lateral knee exhibited the greatest fluctuations [89]. Their working hypothesis suggested that the traditional "heat of wound healing" was more significant laterally and distally, as surgical intervention reduced local perfusion medially [89]. Sharma et al. [90] discovered that the temperature disparity between the operated and non-operated knees persists for several months post-TKA, eventually decreasing to approximately 0.3 °C after one year. An infection may result in a slight increase in knee temperature; both uncomplicated and complicated total knee arthroplasties exhibit an early postoperative temperature elevation, with a modest further increase observed in uncomplicated cases [90]. Although postoperative inflammation is anticipated to produce a thermal pattern characterized by initial diffuse warmth, thermography alone is unable to distinguish between normal and abnormal (possible infection) patterns.

Overall, these observations suggest that, although the pathophysiologic basis underpinning thermographic imaging in arthropathies is broadly shared, principally the association between inflammation, hyperemia, edema, and increased local metabolic activity, the resulting thermal readings are not uniform across disease entities. Rheumatoid arthritis (RA) represents a prototypical example, in which chronic synovitis leads to elevated heat emission over affected joints [49]. However, such thermal changes are not specific to RA, as comparable patterns may be observed in other active arthropathies. Even in osteoarthritis (OA), where inflammation is generally less intense and often low grade, the affected knee may demonstrate a temperature increase of 1–2 °C relative to the contralateral side [16], whereas Charcot neuroarthropathy may produce some of the most marked thermal asymmetries, with inter-limb differences of several degrees [32]. Importantly, these thermographic patterns may also be modulated by disease-specific vascular mechanisms. In psoriatic arthritis (PsA), inflamed joints and entheses are often associated with pronounced vasodilation and preserved thermal responsiveness, whereas in longstanding RA, microvascular dysfunction may paradoxically attenuate heat emission despite persistent inflammatory activity [30,49,81]. Accordingly, thermographic findings should not be interpreted as showing a single universal inflammatory signature, but rather as disease-contextual thermal expressions defined by synovial inflammation, vascular alterations,

edema, and structural tissue remodeling. Within this system, a disease-oriented perspective is essential to define more precisely the clinical relevance of infrared thermography. The following section, therefore, examines its uses across major arthropathies, indicating how these common biological principles translate into distinct diagnostic, phenotypic, and monitoring roles in different clinical contexts.

3.4. Disease-Specific Clinical Applications of Infrared Thermography

3.4.1. Osteoarthritis (OA)

De Marziani et al. [3] reported in a within-patient bilateral knee osteoarthritis cohort (48 men/18 women; mean age 63.3 ± 8.8 years; BMI 25.4 ± 3.2), infrared thermography identified a consistent "heat signature" of symptoms: the symptomatic knee exhibited higher skin temperature than the contralateral asymptomatic knee at the whole-knee level (31.9 ± 1.1 °C vs. 31.6 ± 1.1 °C; $p = 0.003$) with similar results across the assessment of all compartments, with the largest signal in the medial compartment (32.0 ± 1.1 °C vs. 31.7 ± 1.2 °C; $p < 0.0005$) and smaller but significant differences at the patella ($p = 0.015$) and lateral compartment ($p = 0.016$), while the suprapatellar area did not differ (32.0 ± 1.1 °C vs. 31.9 ± 1.1 °C; n.s.). The same group of authors reported also that asymptomatic knees showed comparable medial and lateral temperatures, whereas symptomatic knees demonstrated a medial-dominant pattern (medial > lateral; $p = 0.020$), with the patella remaining the coolest region, while the radiographic severity assessed with these thermal changes: symptomatic knees had higher Kellgren–Lawrence (KL) grades overall ($p < 0.0005$), and when KL grades differed between knees, temperature elevations were observed for total and regional assessments. The authors highlighted that even when KL grades were identical, the medial region retained a significant symptomatic–asymptomatic difference ($p = 0.037$), and the total-knee temperature difference remained significant after adjustment for KL differences ($\Delta \approx 0.225$ °C; $p = 0.002$). Clinically, pain distribution influenced the magnitude of thermal asymmetry: predominant lateral compartment pain was associated with a larger total temperature difference than predominant medial compartment pain (0.7 ± 0.7 °C vs. 0.1 ± 0.5 °C; $p = 0.023$). Although the within-subject design of the study minimizes confounding by age, sex, and BMI, other authors reported that age and BMI can independently influence mean knee skin temperature (Age $p = 0.0003$; BMI $p = 0.02$), with greater OA grade–related variation in younger individuals and a tendency toward lower temperatures at higher BMI within OA grades [3].

Having in mind the fact that OA is steadily acknowledged as encompassing a clinically meaningful inflammatory component and skin temperature is a tractable physical correlate of periarticular inflammation (reflecting local changes in metabolism and vascular supply), infrared thermography can be conceptually leveraged for OA phenotyping by assessing a "high-inflammatory" phenotype that is marked by higher absolute temperatures, compartment-specific hyperthermic patterns over periarticular regions, and greater side-to-side asymmetry aligned with symptom burden from a "low-inflammatory" phenotype, in which thermal elevations are minimal and distributions remain closer to symmetric despite this structural disease [3,21]. This grouping is biologically plausible, but should be validated against objective inflammatory assessments (e.g., ultrasound synovitis/effusion or biomarker panels) to avoid over-attribution of temperature to inflammation alone [3].

There is a small amount of data that assessed a potential "thermal attention threshold" for knee OA. The results are reported in a 2024 scoping review in which the authors derive ≥31.3 °C by aggregating study-level mean knee skin temperatures from 9 included knee OA thermography studies. The mean and median results of this study were both 31.3 °C (SD 1.7 °C), with the middle tercile spanning 31.2–31.5 °C [91]. The same scoping review shows that the underlying temperature distributions overlap substantially with

non-OA comparators and vary by acquisition conditions and participant factors: across included control groups, mean knee temperatures ranged from 25.8 °C up to 31.7 °C (and posterior-view controls ~33.0 °C), while OA means ranged broadly (e.g., 28.7–34.7 °C), alongside marked differences in BMI and study protocols. The authors emphasize that the evidence base is small (only 9 studies) and heterogeneous, with likely confounding (e.g., cutaneous blood-flow variation and OA stage effects, potentially warmer early and colder with progression), so ≥31.3 °C should not be treated as a validated diagnostic cut-off with known sensitivity/specificity.

Regarding the possibility of tracking treatment response in knee OA, the published evidence in the literature indicates that infrared thermography (IRT) has been used to capture treatment-related modulation of superficial joint heat across pharmacologic and rehabilitative interventions. In a placebo-controlled study, the benefit of intra-articular steroid injection was reported as maximal at 1 week and occurred alongside a simultaneous fall in the thermal index, supporting a detectable post-injection anti-inflammatory thermal signal [41]. Also, the same group of authors assessed the possible association with rehabilitation, and concluded that after an acute training session, the exercised knee in OA subjects became significantly warmer than controls, while kinesiology taping in knee OA showed significant improvements in muscle strength and mobility yet no significant change in skin temperature have been detected, suggesting that functional gains can occur independently of a measurable thermographic shift.

In a systematic review, only two IRT-based treatment-outcome studies were identified, one in knee OA and one in TMJ OA, using thermography to monitor response to Movardol (knee OA) and diclofenac sodium (TMJ OA): Movardol supplementation was associated with a significant decrease in thermographically visible "redness" and reductions in both maximum and global mean skin temperature over the affected knee, whereas diclofenac was associated with improved clinical outcomes at 3 months without any measurable change in local temperature, suggesting that analgesic benefit may not also translate into reduced skin thermal output [21].

Reported magnitudes of inter-knee temperature asymmetry across studies requires extended interpretation regarding the study design. Sharma et al. reported an inter-knee asymmetry of around 1.8 °C with a large standardized effect size (d = 2.81) in a comparison of the osteoarthritic knee against the contralateral healthy knee [16], whereas De Marziani et al. reported a much smaller difference of 0.3 °C in a bilateral knee OA study, where the contralateral knee was asymptomatic but radiographically diseased [3]. It is worth noting that there is a six-fold discrepancy. This difference could be due to contrasting a diseased knee with a substantially healthier contralateral knee, which inevitably will yield a larger temperature difference compared to two OA affected knees which differ in symptom status. Thus, these results should always be interpreted within the specific design of the study, to avoid treating results between various studies as comparable.

3.4.2. Rheumatoid Arthritis and Other Inflammatory Arthropathies

In the field of inflammatory arthropathies, infrared thermography produces recognizable thermal patterns that can complement clinical and ultrasound assessment: in cases of rheumatoid arthritis (RA), heat is often distributed in a bilateral or symmetric pattern, such that contralateral temperature differences may be small compared with degenerative cases of disease, consistent with the tendency of RA inflammation to involve paired joints [21]. Regarding the assessment with ITR of the hands, RA-associated hyperthermia is most consistently captured at the MCP and PIP joints, with higher joint temperatures reported in RA versus healthy controls for both MCP and PIP regions [28], and some studies converge on the second/third MCPs and the PIP of the third finger as the most informative targets

for imaging and pattern recognition [21]. Beyond absolute temperature, quantitative descriptors of spatial distribution have also been used, including the Heat Distribution Index (HDI), which discriminated normal from actively inflamed joints and for which an HDI cut-off > 1.3 °C has been reported to correlate with clinically assessed active arthritis [23]. The associations with disease activity are supportive but heterogeneous: older and more recent studies report correlations between thermographic findings and inflammatory/clinical measures (e.g., ESR and/or CRP, and composite clinical scores such as DAS-28/HAQ) [18], whereas other articles report no meaningful relationship between hand temperatures and standard clinical/laboratory activity metrics (including CRP/ESR) [28]. In a 2022 published article that reports the results of a large study using a machine-learning–derived Thermographic Joint Inflammation Score (ThermoJIS), the authors reinforce this nuance: ThermoJIS correlated moderately with ultrasound synovitis scores (grey-scale and power Doppler) and only weakly with laboratory markers (CRP/ESR) and patient-reported/global assessments, suggesting thermography-derived patterns may capture inflammatory information that is closer to imaging than to systemic biomarkers alone [71].

Regarding the use of the technology in the pediatric population (JIA), IRT has been assessed as a screening tool and joint assessment assay (e.g., wrist and knee), with reports of temperature differences between pathological and control joints and correlation with clinical outcomes such as swelling [21]; combined with its non-invasive, non-contact and practical workflow characteristics, this supports its use as a child-friendly adjunct for dynamic evaluation alongside ultrasound rather than a replacement for it [28,71].

3.4.3. Septic Arthritis

IRT is a rapid, non-contact assay that can objectively quantify local hyperthermia as a characteristic of underlying inflammation/infection, published literature from the field orthopedic also supports its possible role in diagnosis of joint infection scenarios mainly through postoperative and periprosthetic joint infection applications rather than native-joint septic arthritis: after total knee arthroplasty, physiological wound-healing inflammation produces a characteristic temperature course, while periprosthetic joint infection can generate a thermographically detectable temperature increase even months after index surgery. What is important to be taken into account is that postoperative diagnostic use is constrained near the surgical field (risk of misinterpreting normal post-surgical hyperthermia), but early trajectories may still help flag impaired wound healing or early infection [89]. A scoping review reports that IRT can be used alone or combined with adjunctive measures (e.g., ESR/CRP) to screen or diagnose suspected infection earlier and guide early intervention [23]. Multiple comparative studies showed that RA-affected joints present higher mean temperatures when compared to healthy controls, which ranges typically between 1.5 °C and 3 °C [34–36,39,58]. This range persists even in patients without symptomatic synovitis, supporting the hypothesis that thermography could detect subclinical inflammation [34–36,39,58]. However, in the reported studies, there is no rigorous selection based on age or other physiological aspects. In contrast with previous results, in cases of native septic arthritis, it is not directly evaluated in the included knee thermography cohorts and appears mainly as an exclusion criterion [41]. In this context, while it is conceptually plausible that marked unilateral “hot-joint” patterns should contribute to emergency triage alongside ultrasound and arthrocentesis pathways, the specific quantitative results would require dedicated prospective validation in suspected septic arthritis populations before workflow integration.

A series of cross-sectional studies from one research group has assessed the correlation between thermography and ultrasounds using the same setup (thermal camera FLIR T640/T865). Across several joints (wrist, elbows, interphalangeal, and metacarpopha-

langeal) the temperature correlated with the ultrasound grey-scales (r around 0.3–0.5) and more strongly with power Doppler scores (r around 0.4–0.6) with an ICC over 0.99 [47–54,56,84]. However, all the studies share the same limitation: the ROI placement is done manually, and no longitudinal treatment-response data, which limits the use of their data for clinical application, especially for monitoring disease progression.

3.4.4. Juvenile Idiopathic Arthritis

The evidence regarding thermography in juvenile idiopathic arthritis (JIA) remains limited but supports the use of this non-invasive technology as an adjunctive tool to detect clinically active joint inflammation of the wrist, knee, and ankle. Lerkvaleekul et al. demonstrated higher mean and maximum wrist temperature in children with active arthritis of the wrist compared with JIA children without and healthy children; diagnosis sensitivity and specificity are highest in the assessment of moderate to severe arthritis: Tmean 31.0 °C (sensitivity 85.7%, specificity 80.0%) and Tmax 32.3 °C (sensitivity 71.4%, specificity 93.3%) [40]. Nwaizu et al. reported increased thermal signature in knees with active JIA compared to quiescent knees (median values 31.30 vs. 30.33 °C, $p = 0.0078$); thermography correlated with subjective color visualization in 16 of 20 participants and may therefore offer some support in the objective evaluation of knee joint inflammation [43].

The most significant methodological contribution to thermography has come from Zhao et al., which describes the temperature derived after within-limb calibration (TAWiC) using the ipsilateral mid-tibial surface as an internal reference; this technique results in better diagnostic performance compared with raw temperature, with AUC values up to 0.867 and high specificity (0.90) at the knee joint [60]. Recently, Siddiqui et al. demonstrated that using a smartphone for thermal imaging could distinguish affected pediatric joints at the knee and ankle from healthy children and affected from unaffected contralateral joints, yielding AUCs of 0.94 at the knee and 0.91 at the ankle when cutoffs for T-avg are at 31.5 °C and 31.1 °C, respectively [45]. Generally, pediatric studies of thermography suggest that this is a rapid, child-friendly tool for screening and monitoring of JIA, especially when calibrated against internal reference regions, but limited cohort sizes, mixed diagnoses among pediatric rheumatological conditions, varied definitions of active disease, and a limited number of longitudinal studies correlating findings with ultrasound or MRI represent significant limitations.

3.4.5. Post-Arthroplasty and Periprosthetic Complications

After TKA, infrared thermography/telethermography can provide an objective, non-contact "thermal recovery curve" and may flag deviations suggestive of complications such as periprosthetic joint infections. Because postoperative thermal patterns are also influenced by the extent of surgical exposure and soft-tissue handling, interpretation of peri-incisional hyperthermia should be made in the context of the surgical approach used during TKA [92]. In uncomplicated TKA, a reproducible postoperative pattern has also been described in the published literature, with a steep early rise in operated-vs-contralateral temperature asymmetry peaking around postoperative day 3 (mean differential temperature 3.4 ± 0.7 °C), followed by a gradual normalization by ~2–3 months (0.5 ± 1.3 °C at 60 days; -0.1 ± 1.1 °C at 90 days) and stability thereafter [93]. Adding to these single-cohort observations, a systematic review/meta-analysis quantified the expected ΔST pattern in uncomplicated cases (highest within the first 2 weeks, pooled ΔST ≈ 2.8 °C; ~1.4 °C at 3 months; ~0.9 °C at 6 months; ~0.6 °C at 12 months, approximating preoperative levels), supporting the idea that persistent or secondary temperature elevation beyond the anticipated time course warrants closer assessment [94]. What should also be taken into account is that regional perfusion effects can confound interpretation near the surgical approach: after TKA, the

area of greatest surgical trauma (medial parapatellar region) may show little early temperature increase due to local perfusion compromise, whereas more distant or lateral area better reflect physiological wound-healing hyperemia, thereby limiting immediate postoperative diagnostic use to areas away from the incision [89]. In suspected cases of periprosthetic joint infection, telethermography has shown discriminatory potential months after surgery (e.g., local increases of ~1.1–2.5 °C reported in septic cases), and a prospective cohort using digital telethermography reported diagnostic performance for knee PJIs with accuracy 0.90, sensitivity 0.89, and specificity 0.91 [93]. Overall, thermal imaging is best positioned as an adjunctive screening or monitoring modality, particularly for serial follow-up and early triage, rather than a standalone test, given postoperative inflammation/perfusion artifacts and the need to integrate established PJI workups.

3.4.6. Quantitative Thermography and Imaging Analytics

Quantitative IRT is increasingly shifting from qualitative "hot/cold" inspection toward reproducible, ROI-driven metrics as well as higher-order spatial descriptors. Throughout various musculoskeletal applications, the most commonly reported parameters remain mean, maximum, and minimum skin temperature within predefined regions of interest (ROIs), alongside differential measures such as side-to-side temperature differences (ΔT) and intra-ROI contrasts (e.g., Tmax–Tmin) to reduce inter-individual variability and highlight focal inflammation [57,95]. ROI definition and extraction are a major determinant of analytic robustness; while early studies relied on manual or geometric ROIs, more recent work describes automated segmentation approaches (e.g., color-based segmentation) to improve exactness and throughput for knee OA thermograms [41]. Specific segmentation methods have been designed for inflammation-affected knee thermograms. RASIT framework, a method that uses electrostatic-force image computation to create a "region-shrunk" segmentation, reached an accuracy of 98.2% and Dice Similarity Coefficient (DSC) of 0.805 when tested on 50 arthritic knee images [64]. The limitation of this study is in calculating the accuracy, given that the automated step needed a previous manual crop processing, which limits the feasibility of clinical usage, and also the low number of images. Moreover, other anatomical regions (breast) thermograms were used, which could affect the knee-specific results [64]. Similar segmentation frameworks specifically designed for an inflammation-affected knee were reported: either extended region-growing with logarithmic transformation and multi-seed selection, which has a DSC of 0.790 and accuracy of 98.1% [66], or cluster-ensemble segmentation that reported a pixel accuracy of 98% [67].

Beyond point summaries, "thermogram biomarkers" that encode heat distribution and spatial organization are being adopted, including the Heat Distribution Index (HDI), reported to discriminate active arthritis from controls with an HDI cut-off of 1.3 °C [23], as well as heat gradients, symmetry/asymmetry patterns, and pixel-based descriptors such as the proportion of an ROI exceeding a predefined temperature band (useful for capturing diffuse vs. focal hyperthermia) [41,96]. Machine learning and deep learning methods build on these quantitative features by enabling automatic preprocessing plus ROI extraction, thermogram classification (e.g., disease activity/severity strata), and scalable decision-support [97]; notably, a large rheumatology dataset was used to develop a machine learning–derived ThermoJIS that detected ultrasound-defined active synovitis and was higher in "clinical remission" when subclinical synovitis persisted, supporting multimodal fusion with ultrasound and biomarkers rather than redundancy [71].

3.5. Clinico-Imaging Correlations

Thermography displays substantial potential as an alternative to established clinical and imaging indicators of inflammation, which is notably appealing to individuals with

arthritis. Numerous research studies have examined the correlation between temperature observations and clinical indices, ultrasonography, and biomarkers, producing largely positive outcomes. Power Doppler ultrasonography, which directly visualizes synovial blood flow, and thermography have shown notable connections. Morales et al.'s automated Thermographic Joint Inflammation Score (ThermoJIS) exhibited a moderate correlation with grey-scale synovial hypertrophy (Spearman $\rho = 0.49$) and power Doppler grade ($\rho = 0.51$) in patients with rheumatoid arthritis as assessed by ultrasonography [71]. Tan et al. also discovered, as previously noted, that temperature measurements were significantly elevated in RA joints that were tested positive for ultrasound-synovitis compared to those which were tested negative. The correlations between joint temperature and semiquantitative ultrasound assessments are modest yet statistically significant, with r values between approximately 0.4 to 0.5 [52]. Notably, thermography can detect inflammation even in clinically "silent" joints. Tan et al. established a correlation in the same study between total ultrasonography inflammatory scores and the aggregate temperatures of MCP joints (r ~0.42–0.47) [52], even in hands that appeared clinically quiescent (neither swollen nor tender). Thermography, akin to other sophisticated imaging modalities, appears to be sensitive to subclinical synovitis. A strong link exists between inflammation and joint temperature, as demonstrated in numerous studies.

There are correlations between thermographic data and conventional clinical and laboratory indicators; however, the intensity of these linkages differs. Convincing evidence links inflammation to serological markers, particularly in larger joints. Snekhalatha et al. [76,77] discovered a solid correlation between skin temperature and erythrocyte sedimentation rate (ESR) in their investigations of rheumatoid arthritis (RA) knees. They found that ESR was similarly linked with knee thermal parameters (e.g., mean temperature) as with radiographic evaluations of joint deterioration [76]. A follow-up study conducted by the same team, which incorporated thermal and Doppler ultrasonography features, revealed a solid correlation among thermal characteristics and both erythrocyte sedimentation rate (ESR) and C-reactive protein (CRP) levels in patients with rheumatoid arthritis (RA) [77]. As ESR/CRP levels increased, the "thermal index" and the average skin temperature of the knees also rose. Thermography appears to have precisely quantified the degree of physiological inflammation in this post-surgical context, as evidenced by the substantial correlation. The association between CRP and non-surgical chronic arthritis is probably less robust than that with local imaging, despite the identification of some important correlations [98]. It is evident that significant inflammation typically elevates systemic indicators, subsequently increasing joint temperature. In contrast, local causes are more likely to account for thermographic anomalies when CRP and ESR levels are within normal ranges [82].

Correlation with clinical exam and composite disease indices shows promise while also highlighting thermography's limitations. Two novel composite indices, ThermoDAI and ThermoDAI-CRP, were developed to enable physicians to monitor rheumatoid arthritis patients remotely. In this case [72], these measures integrate thermographic evaluations with patient global assessment and C-reactive protein (CRP). Spearman $\rho > 0.83$–0.85 [72] indicates that the indices using thermography closely resemble the conventional disease activity assessments (CDAI, SDAI, DAS28). The correlation between ThermoDAI and ultrasonography synovitis scores was much stronger than that of patient global assessment alone or patient global assessment combined with CRP [72]. This indicates that the incorporation of objective thermal data enhanced image alignment more effectively than relying just on subjective or laboratory assessments. Tan et al. [51] discovered that the combination of thermography and a basic clinical joint evaluation (swelling/tenderness) identified a greater number of joints with ultrasound-verified inflammation compared to the use of

thermography in isolation. Ultrasound-detected synovitis was observed in several joints, and their "integrated thermal and clinical evaluation" approach boosted sensitivity for these cases [51]. The data show that thermography is most efficacious when employed with clinical evaluation rather than as a replacement. A patient displaying discomfort and swelling upon examination, along with warm joints identified through thermography, is likely to show authentic inflammation on imaging [51].

Nevertheless, there are certain distinctions. Jones et al. found no association between average hand joint temperature and clinical disease activity evaluations in rheumatoid arthritis (RA), a result that warrants caution. Neither DAS28 scores, swollen joint counts, nor HAQ disability scores showed any clear relationship to thermal data in their cohort [39]. The study also showed no correlation between CRP or ESR and joint temperature. Then, one important question arises: What factors result in such discordant findings? One reason may be potential methodological bias: Jones et al. calculated the average temperatures across all hand joints, which may have attenuated the signal from the highly inflammatory joints (a limited number of hot joints among several moderately warm ones could have reduced the overall average). Conversely, Tan and Morales analyzed each joint separately or employed methods that indicated the warmest areas [49,72]. Furthermore, the average disease activity in the RA patients from Jones's study was rather low, and the reduced camera resolution may have obscured subtle variations. Therefore, the limited associations observed in previous RA hand studies using more in-depth analyses should not be disregarded, despite their finding that thermography "does not seem to be effective for small joints of the hand" in isolation [39]. However, it likewise emphasizes that there are instances when a direct correlation between joint temperature and clinical manifestations is not always evident. An orderly association may be interrupted because of factors such as environmental conditions (humidity, temperature, acclimatization) [99], drugs (vasoconstrictors, vasodilators, corticosteroids) [100], or the presence of concomitant Raynaud's phenomenon, peripheral arterial disease, or diabetic angiopathy [101–103].

Moreover, there is limited evidence of a link between osteoarthritis and other non-rheumatoid arthritic conditions; yet, it indicates that thermography may provide valuable therapeutic insights. Research suggests that in cases of knee osteoarthritis, increased thermal asymmetry correlates with worsened pain and functional evaluations. In contrast, temperature data seem to show a reduced correlation with subjective pain compared to objective findings [16]. This dissociation has practical significance, as heat indicates inflammation; nevertheless, a patient may not perceive it as pain, implying ongoing pathology (such as growing joint degradation or an approaching flare) prior to the manifestation of major symptoms [16].

3.6. Diagnostic Pathways: Where Does Thermography Fit?

One essential consideration as infrared thermography transitions from the laboratory to clinical settings is its power to enhance the identification and surveillance of arthropathies. Recent research shows that thermography is most effective when combined with conventional clinical and imaging data; it performs as a swift, advantageous supplementary method with particular benefits. Thermography provides multiple advantages, including its non-invasive nature, rapid acquisition, and ability to assess multiple joints simultaneously without radiation [40,45]. Acquiring a comprehensive thermal image of the hand, for instance, requires a few seconds and provides an immediate "map" of potential inflammation. This renders it appealing for regular use in clinics or in remote telemedicine contexts where usual imaging methods, such as ultrasound or MRI, are impractical. Morales-Ivorra et al. suggest that thermography has the capacity to revolutionize rheumatologists' techniques for detecting joint inflammation. This technique may assist

in perceiving subtle disease activity [71,72]. Thermal imaging may assist in excluding any residual inflammation; for example, a rheumatoid arthritis patient appearing to be in remission could have their joints assessed for any persistent "hot" spots; if such spots are present, further ultrasonography or an alteration in treatment may be required [71,72].

Thermography is utilized in telemedicine and remote monitoring. During the COVID-19 epidemic, there was a significant increase in interest in remote examinations for arthritis. Furthermore, patient-operated thermographic imaging has demonstrated unexpectedly advantageous results. Wong et al. (2025) employed a rudimentary infrared camera attached to a smartphone to observe inflammation in the knees of teenagers afflicted with arthritis [86]. Images captured by monitoring parents at home showed no differences when compared to those taken in a clinical environment, confirming the feasibility of collecting thermal data in a domestic setting [86]. The application of a calibrated temperature differential, known as the TAWiC metric, for detecting active arthritis proved equally effective in both clinical and home environments, exhibiting a sensitivity of approximately 0.44 and a specificity of around 0.79 in their pilot study [86]. This signifies a potential future scenario where patients routinely provide thermal photos of their joints, and clinicians evaluate which individuals require additional investigation based on those photographs. Based on this concept, Morales-Ivorra's team developed the ThermoDAI, a disease activity index for rheumatoid arthritis that correlates with ultrasonography and composite assessments [72]. It integrates self-reported global scores with machine learning analysis of hand thermograms. A patient can upload their hand thermogram from home to obtain an objective disease activity index (ThermoDAI) comparable to the findings of a DAS28 test conducted in a clinical setting [72]. Consequently, thermography may emerge as an important part of tele-rheumatology, facilitating standardized and objective joint evaluations remotely.

In day-to-day diagnostics, where might thermography "fit" in the workflow? It may serve as a screening instrument in primary care or clinics that detect arthritis at an early stage. A rapid thermographic assessment of the hands and knees may be conducted on patients exhibiting diffuse arthralgias. If the images reveal distinct hot spots or irregular heat distribution, it would indicate inflammatory arthritis, in contrast to fibromyalgia, which lacks localized heat. Sharma et al. contend that thermal imaging serves as an effective method for ruling out or screening for arthritis due to its great sensitivity [16]. Despite variations in specificity, other validation investigations have determined thermal imaging sensitivities ranging from 60% to 95% [40,45,63,68]. If the thermogram displays no significant temperature variations, it may be prudent to reassure the patient or deprioritize inflammatory disease as a concern. If the thermogram is abnormal, additional high-yield testing should be conducted. This may result in some false positives while lowering false negatives. Due to its limited specificity, thermography should not serve as a definitive diagnosis. Rather, it needs to be utilized to initiate additional testing to verify the patient's condition. Figure 3 depicts a conceptual diagnostic and monitoring pathway that incorporates infrared thermography, supporting the application of these methods in clinical environments.

The application of AI for the complete automation of thermogram diagnostics is a rapidly progressing subject. The convergence of AI and flexible or wearable sensing technologies is expected to accelerate the translation of thermography into accessible workflows, supporting remote assessments in resource-limited settings [104]. Ahalya et al. trained two neural networks (one custom convolutional and one quanvolutional) on 600 hand thermograms from 50 RA patients and 50 healthy controls, acquired with a FLIR A305SC camera (around 1440 images) under controlled conditions (20 °C, 15 min acclimatization, 1 m distance) [61]. They were accurate approximately 95% to 97% of the time [61]. The limitation of this study was the lack of external validation; they should be

interpreted accordingly. In another study that uses the same set-up and same conditions, classical machine-learning are compared to quantum support vector machines (QSVMs) for identifying joints affected by RA (a smaller lot of 30 RA patients and 30 controls) [62]. Lower accuracies were reported compared to the previous study and the same limitation of no external validation can also be mentioned here, along with a smaller patients cohort [62]. Beyond image-based workflows, Pauk et al. developed an artificial neural network (ANN) utilizing a synthesis of clinical and thermal data [74]. They achieved an overall accuracy of 93% when distinguishing rheumatoid arthritis (RA) from healthy persons, with a sensitivity of 81% and a specificity of 100% in their test cohort [74]. They propose that thermographic data, in conjunction with other clinical characteristics, can be employed to screen for, diagnose, and monitor rheumatoid arthritis together with established criteria.

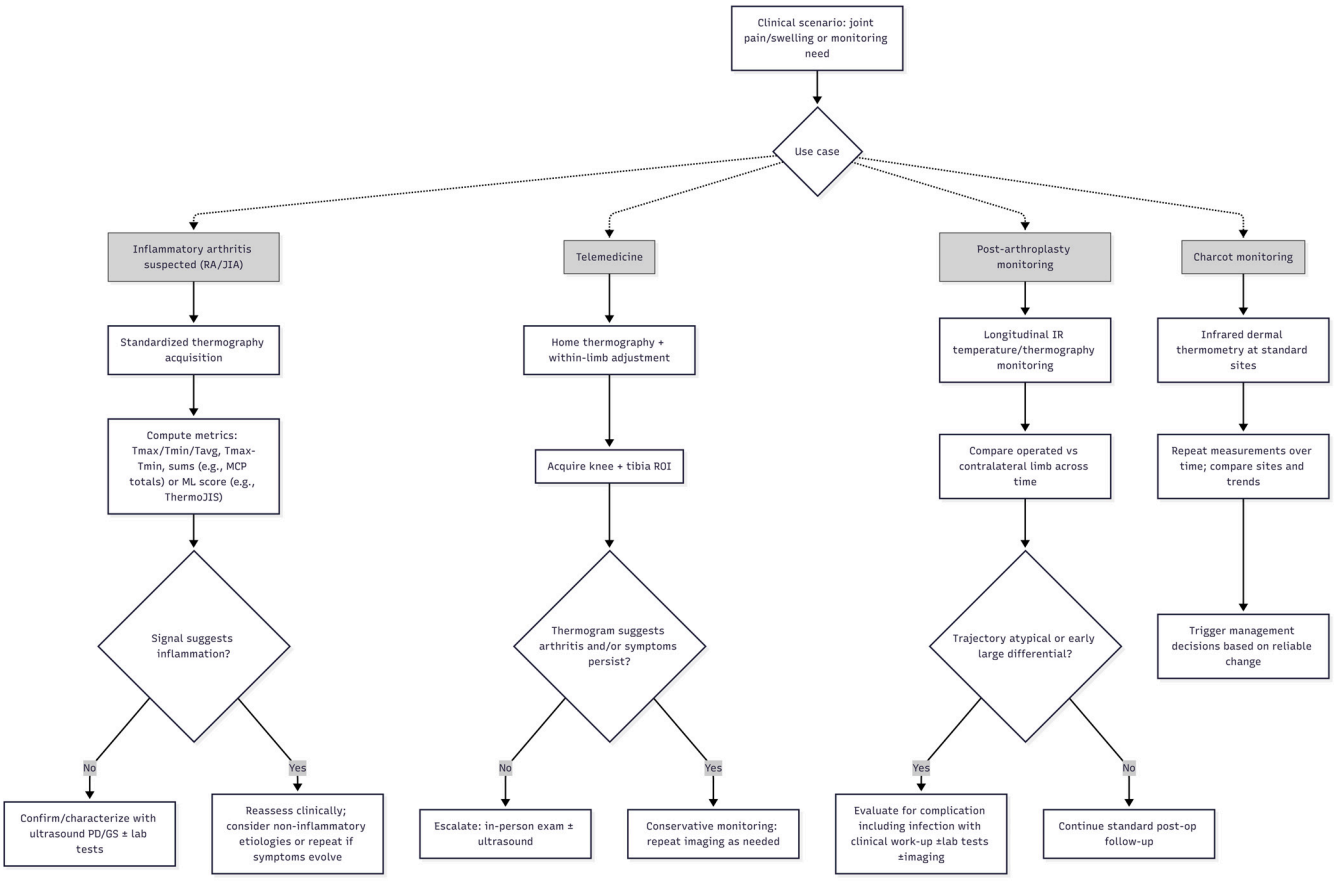

Figure 3. Conceptual clinical workflow for the integration of infrared thermography in arthropathy diagnosis and monitoring.

Another group interpreted the thermograms recorded after 70% isopropyl-alcohol cooling instead of cold water (100 patients in total: 70 with RA, and 30 healthy controls) of the hands. Given the reported T-cooling (0.025) and T-rewarming (0.042), it contradicts the hypothesis that alcohol influences the thermographies due to heat caused by alcohol-induced local vasodilation [65]. Although challenges remain, such as determining the concentration of the alcohol used, or the pharmacological effects that it can produce, using this method of cooling could represent a good alternative for patients that cannot immerse their hands in cold water, given that the accuracy is similar to previously reported results in this review (93% accuracy with SVM) [65]. Several other studies used classical machine learning pipelines: Morales-Ivorra et al. developed and validated the Thermographic Joint Inflammation Score (ThermoJIS), showing a strong correlation with ultrasound-detected synovitis, and achieved an AUROC of 0.78 for detecting active inflammation [71].

Bardhan and Bhowmik applied texture-based features and support vector machines (SVMs) to 110 knee thermal images acquired with a FLIR T-650sc camera, with different conditions compared to the previous Ahalya et al. two studies (0.02 °C sensitivity at 30 °C; 22 °C dark room and same time-frame acclimatization), yielding 93% sensitivity [63]. It is worth noting that when comparing non-arthritis knees to affected ones, a 91% accuracy is reported, and only 73% when comparing RA knees with other arthritides. However, the reported accuracy of 73% could be inaccurate due to the low set for this stage (only 20 RA thermograms) [63]. Similar results were reported by Das et al., who used random forest, SVM, and k-nearest neighbor on pixel-wise features to classify knee arthritis with >90% accuracy [68].

Publicly available datasets can also be used. A group of authors developed a hybrid pipeline on the publicly available Infrared Knee Joint Dataset, where modified K-means segmentations were combined with handcrafted-image-derived features, which were interpreted as a hyaluronic-acid proxy (an accuracy of 96.4% were achieved) [68]. This study is one of the few that uses publicly available images, ensuring the possibility for reproducibility and generability [68]. Worth mentioning, despite being a small single-center dataset with no external validation, not early or at-risk RA, and a small cohort (100 patients: 50 RA and 50 controls) is a study that reported thermal imaging that outperformed radiographs [69]. Using thermal-image by color-based k-means clustering for hot-spot segmentation and SURF feature extraction, an accuracy of 93.75% (QSVM) was reported and 92.5% (RA-XTNet), higher when compared with radiographs, where the same machine learning pipeline was applied [69]. These results should be confirmed with larger, multi-center cohorts. However, it is the first proof that thermal imaging can perform better in specific pipelines when assessing RA-affected hands, which holds clinical value.

4. Discussion

Infrared thermography is progressively acknowledged as a significant technique for detecting inflammation in joints associated with arthropathies. Inflammation's ability to generate heat represents a fundamental concept in pathophysiology, which underpins its significance. Inflamed joints emit greater levels of infrared radiation compared to normal joints. This indicates inflammatory arthritic conditions, such as rheumatoid arthritis (RA), psoriatic arthritis (PsA), and osteoarthritis (OA), as well as neuropathic disorders, such as Charcot arthropathy. This is the biological rationale for thermography's efficacy. In chronic rheumatoid arthritis (RA), vascular rarefaction may cause joints to appear cold despite being warm. In Charcot foot, neuropathic circulation has the ability to amplify thermal signals. Although heat is a prominent indicator of inflammation, its absence does not rule out the presence of a disease.

Given the ability of machine learning algorithms to detect subtle imaging patterns [105,106], similar approaches could be applied to thermographic data to enhance diagnostic accuracy. Thermal imaging today focuses on obtaining dependable, reproducible temperature measurements utilizing high-resolution, full-field cameras and automated processing techniques. To minimize variation, it is essential to implement appropriate environmental controls, imaging methodologies, and anatomical uniformity. Despite improvements in inter-operator reliability through training and observance of guidelines, achieving consensus among studies and sites continues to be difficult. Consequently, imaging techniques, ROI delineations, and data interpretation standards remain under development. The approach possesses notable potential for reproducibility; however, it has to be meticulously adhered to in both clinical and research conditions to be effective.

Thermographic patterns illustrate the appearance of inflammation throughout the body. Rheumatoid arthritis (RA) is defined by unilateral and polyarticular increases in

temperature. Osteoarthritis (OA) is more prone to induce localized joint warmth, particularly in the knee. Charcot foot is characterized by generalized warmth in the foot, whereas psoriatic arthritis (PsA) may induce warmth in the entire digit or at the enthesis. Caution must be exercised when seeing localized warmth following surgery, such as TKA. Numerous investigations have shown that thermographic "hot joints" are associated with inflammation, as verified by ultrasonography or physical examination. Measuring surface temperature may occasionally overlook slight or deep inflammation. To prevent erroneous diagnoses, thermograms must be interpreted with consideration of the distinctive patterns and confounding factors associated with the illness.

Correlation assessments indicate that thermographic signals are generally congruent with other indicators of inflammation. Thermographic abnormalities are most clinically meaningful when they correspond with independent indicators of inflammation, such as clinical swelling or tenderness, elevated inflammatory biomarkers, grey-scale ultrasound synovitis, or power Doppler signal. During active inflammation, thermography correlates with elevated CRP/ESR levels. Nonetheless, there exists a possibility of discord when the disease is in its early phases or is confined. This reinforces the consensus that thermography should be regarded as a supplementary biomarker to be utilized with other diagnostic methods, such as ultrasonography, laboratory tests, and clinical assessment. Individuals are more inclined to trust thermography results when they correspond with other findings. When they fail to do so, they call for additional research.

The negative result reported by Jones et al. [39] should be considered genuine evidence rather than being categorized as inferior results. In their group of patients, with diagnosed RA, but low-activity, the hand thermographies failed to differentiate between active and inactive disease, and no correlation was found regarding CRP, ESR, or swollen joint counts. These results could have been influenced by the low-resolution camera, or the low activity of the disease [39]. Considering the translation to general use of the IRT in clinical practice, we can infer that thermography has limited diagnostic value at the small joints of the hand in low-activity disease, and that its performance is most reliable in joints with moderate to severe synovitis or in larger joints, where the heat output is increased.

Thermography possesses considerable potential; however, it must overcome multiple challenges before it can be effectively included in diagnostic protocols. A major problem is the inconsistency among the facilities. If each clinic employs distinct methods for calibrating cameras, arranging rooms, or delineating ROI, the outcomes may vary. Literature frequently advocates for uniform methodologies to ensure a uniform comprehension of what constitutes a "positive" thermal discovery. It is important to ensure that all study organizations adhere to the same protocols, like the duration required for acclimatization or the effects of a ΔT of X. Another issue is making sure that medical workers are capable of correctly assessing the information. Thermography produces an image that requires interpretation, whereas other laboratory procedures provide binary results. Rheumatologists or AI systems must acquire the ability to precisely interpret these images to prevent typical variations in vascularity from being misidentified as pathological conditions. Physiological variables may occasionally result in false negatives if caution is not used. Individuals with peripheral vascular disease or those utilizing vasoconstrictive medications may consistently exhibit colder skin, perhaps obscuring signs of inflammation. An individual with a fever or systemic vasodilation may have excessive joint signals caused to elevated skin temperature, possibly resulting in false positives. Sharma et al. assert that the low specificity of thermography may result in false positives when other factors induce skin heating. A warm knee post-surgery may indicate an infection or may not. A thorough study revealed that temperature alone is an inadequate indicator of infection in TKA, since infected knees were

only roughly 0.27 °C warmer than normal ones after two weeks. The clinical context is important for interpreting thermography results.

Finally, cost and usefulness must be mentioned. High-quality IR cameras remain costly, though their prices have been dropping over the past few years as they become more common. Conversely, inexpensive infrared (IR) accessories for cellphones are beginning to emerge [107]. This may facilitate their access and utilization in resource-poor environments. A portable, battery-powered thermal camera may be utilized in a rural clinic as an "imaging modality." This could be highly advantageous in areas without access to MRI or ultrasound. Due to its rapid results and absence of ionizing radiation, it is reusable, permitting immediate decision-making throughout treatment. We anticipate that, in the future, thermography will become as simple as "scan the joint, obtain a score," facilitated by computer analysis. This will function effectively in high-volume clinics without imposing excessive demand on them.

Translating IRT results discussed in this review to clinical practice will depend on the how a standard in this technology will be designed and implemented in the clinics. A clear acclimatization period should be implemented and used across all studies (for example, 15 min as reported in the majority of the original studies), an ambient temperature (around 20 °C) with a stable humidity, and consecutive reporting of these values. A standard should be implemented in the technology and the technical specification of the camera that are used in terms of resolution, thermal sensitivity, lens properties; also, distance to the patients should be standardized. Moreover, manual ROI placement should be replaced with semiautomated or automated methods. Interpreting the results with a multidisciplinary team could also help with the future use of IRT in clinic.

Limitations of the Present Review

Several limitations of the review should be acknowledged. The literature search was performed in PubMed, Scopus, and Web of Science, additional databases such as Embase, Cochrane Library, were not searched, thus relevant thermography literature could have been underrepresented. Moreover, because the search was limited to English-language publications, some relevant papers could have been excluded. No risk-of-bias was applied to the included studies, all the studies were assessed only qualitatively, thus resulting in a more subjective view of the articles that were reviewed.

5. Conclusions

Infrared thermography is a beneficial additional imaging technique for arthropathies, especially because it can detect functional thermal changes associated with inflammation, hyperemia, vascular remodeling, and local metabolic activity. Thermography consistently identified clinically significant temperature changes across osteoarthritis, rheumatoid arthritis, juvenile idiopathic arthritis, Charcot neuroarthropathy, and post-arthroplasty contexts, frequently associating with ultrasound results, inflammatory markers, or symptom burden. Its main advantages are that it is quick, inexpensive, and non-invasive, and that it can be used at the bedside, for serial monitoring, or in telemedicine. At the same time, improvements in quantitative thermal analysis, automated segmentation, and artificial intelligence are making it more accurate and opening new ways to conduct remote screenings and support decision-making.

The existing literature suggests that thermography should not yet be regarded as an independent diagnostic modality. Its performance continues to be affected by methodological variability, surrounding factors, vascular confounders, and variations in disease phenotype, anatomical location, and acquisition protocol. Before imaging can be widely used in clinical settings, it is important to standardize the conditions, region-of-interest selection,

calibration methods, and interpretation criteria. In general, infrared thermography is a very useful addition to multimodal diagnostic pathways in rheumatology, orthopedics, and rehabilitation. Future progress will likely depend on regulated protocols, larger prospective validation studies, and better integration with clinical, laboratory, and conventional imaging data.

Author Contributions: Conceptualization, C.-A.A., S.D., C.C. and C.S.; methodology, C.-A.A., A.-G.G. and A.-E.M.; validation, I.-A.T., S.D., R.-M.B., A.I., C.S. and C.C.; formal analysis, A.-G.G., I.-A.T., C.A., Ł.P. and M.E.G.; investigation, C.-A.A., R.-M.B., A.-E.M., M.E.G. and A.I.; resources, C.S., C.C. and R.C.; data curation, A.-G.G., I.-A.T., C.A. and Ł.P.; writing—original draft preparation, C.-A.A., S.D., A.-G.G., I.-A.T., R.-M.B., C.A., A.-E.M., M.E.G., Ł.P., A.I., R.C., C.C. and C.S.; writing—review and editing, S.D., R.C., C.C. and C.S.; supervision, C.C. and C.S. All authors have read and agreed to the published version of the manuscript.

Funding: This research received no external funding.

Institutional Review Board Statement: The study was conducted in accordance with the Declaration of Helsinki and was approved by the Institutional Ethics Committee of "Foișor" Clinical Hospital for Orthopedics, Traumatology and Osteoarticular TB (no. 1024 from 18 February 2026).

Informed Consent Statement: Informed consent was obtained from all subjects whose thermal images were used in the study.

Data Availability Statement: No new data were created or analyzed in this study. Data sharing is not applicable to this article.

Conflicts of Interest: The authors declare no conflicts of interest.

References

1. Li, H.Z.; Liang, X.Z.; Sun, Y.Q.; Jia, H.F.; Li, J.C.; Li, G. Global, regional, and national burdens of osteoarthritis from 1990 to 2021: Findings from the 2021 global burden of disease study. *Front. Med.* **2024**, *11*, 1476853. [CrossRef]
2. Steinmetz, J.D.; Culbreth, G.T.; Haile, L.M.; Rafferty, Q.; Lo, J.; Fukutaki, K.G.; Cruz, J.A.; Smith, A.E.; Vollset, S.E.; Brooks, P.M. Global, regional, and national burden of osteoarthritis, 1990–2020 and projections to 2050: A systematic analysis for the Global Burden of Disease Study 2021. *Lancet Rheumatol.* **2023**, *5*, e508–e522. [CrossRef]
3. De Marziani, L.; Zanasi, L.; Roveda, G.; Boffa, A.; Andriolo, L.; Di Martino, A.; Zaffagnini, S.; Filardo, G. Symptoms and joint degeneration correlate with the temperature of osteoarthritic knees: An infrared thermography analysis. *Int. Orthop.* **2025**, *49*, 101–108. [CrossRef]
4. Lembke, S.; Macfarlane, G.J.; Jones, G.T. The worldwide prevalence of psoriatic arthritis-a systematic review and meta-analysis. *Rheumatology* **2024**, *63*, 3211–3220. [CrossRef]
5. Momodu, I.I.; Savaliya, V. Septic Arthritis. In *StatPearls*; StatPearls Publishing: Treasure Island, FL, USA, 2026.
6. Hunter, D.J.; Bierma-Zeinstra, S. Osteoarthritis. *Lancet* **2019**, *393*, 1745–1759. [CrossRef]
7. Dragosloveanu, S.; Petre, M.-A.; Gherghe, M.E.; Nedelea, D.-G.; Scheau, C.; Cergan, R. Overall Accuracy of Radiological Digital Planning for Total Hip Arthroplasty in a Specialized Orthopaedics Hospital. *J. Clin. Med.* **2023**, *12*, 4503. [CrossRef]
8. Lee, L.S.; Chan, P.K.; Fung, W.C.; Chan, V.W.K.; Yan, C.H.; Chiu, K.Y. Imaging of knee osteoarthritis: A review of current evidence and clinical guidelines. *Musculoskelet. Care* **2021**, *19*, 363–374. [CrossRef]
9. Guermazi, A.; Roemer, F.W.; Hayashi, D. Imaging of osteoarthritis: Update from a radiological perspective. *Curr. Opin. Rheumatol.* **2011**, *23*, 484–491. [CrossRef] [PubMed]
10. Piccolo, C.L.; Mallio, C.A.; Vaccarino, F.; Grasso, R.F.; Zobel, B.B. Imaging of knee osteoarthritis: A review of multimodal diagnostic approach. *Quant. Imaging Med. Surg.* **2023**, *13*, 7582–7595. [CrossRef] [PubMed]
11. Zufferey, P.; Tamborrini, G.; Gabay, C.; Krebs, A.; Kyburz, D.; Michel, B.; Moser, U.; Villiger, P.M.; So, A.; Ziswiler, H.R. Recommendations for the use of ultrasound in rheumatoid arthritis: Literature review and SONAR score experience. *Swiss Med. Wkly.* **2013**, *143*, w13861. [CrossRef] [PubMed]
12. Ansar, W.; Ghosh, S. Inflammation and Inflammatory Diseases, Markers, and Mediators: Role of CRP in Some Inflammatory Diseases. In *Biology of C Reactive Protein in Health and Disease*; Springer: New Delhi, India, 2016; pp. 67–107. [CrossRef]
13. Szekanecz, Z.; Koch, A.E. Mechanisms of Disease: Angiogenesis in inflammatory diseases. *Nat. Clin. Pract. Rheumatol.* **2007**, *3*, 635–643. [CrossRef] [PubMed]
14. Firestein, G.S. Evolving concepts of rheumatoid arthritis. *Nature* **2003**, *423*, 356–361. [CrossRef]

15. Lahiri, B.B.; Bagavathiappan, S.; Jayakumar, T.; Philip, J. Medical applications of infrared thermography: A review. *Infrared Phys. Technol.* **2012**, *55*, 221–235. [CrossRef]
16. Sharma, M.K.; Sood, H. Infrared thermal imaging as a non-invasive pre-diagnostic tool for knee osteoarthritis: A cross-sectional study. *J. Therm. Biol.* **2025**, *133*, 104281. [CrossRef]
17. Crisafulli, D.; Spataro, M.; De Marchis, C.; Risitano, G.; Milone, D. A New Sensorized Approach Based on a DeepLabCut Model and IR Thermography for Characterizing the Thermal Profile in Knees During Exercise. *Sensors* **2024**, *24*, 7862. [CrossRef]
18. Cosoroaba, M.R.; Cirin, L.; Anghel, M.D.; Talpos-Niculescu, C.I.; Argesanu, V.; Farkas, A.Z.; Negrutiu, M.L. The use of thermal imaging in evaluating musculoskeletal disorders in dentists. *J. Med. Life* **2019**, *12*, 247–252. [CrossRef]
19. Dragosloveanu, S.; Capitanu, B.S.; Josanu, R.; Vulpe, D.; Cergan, R.; Scheau, C. Radiological Assessment of Coronal Plane Alignment of the Knee Phenotypes in the Romanian Population. *J. Clin. Med.* **2024**, *13*, 4223. [CrossRef] [PubMed]
20. Liu, Q.; Li, M.; Wang, W.; Jin, S.; Piao, H.; Jiang, Y.; Li, N.; Yao, H. Infrared thermography in clinical practice: A literature review. *Eur. J. Med. Res.* **2025**, *30*, 33. [CrossRef]
21. Schiavon, G.; Capone, G.; Frize, M.; Zaffagnini, S.; Candrian, C.; Filardo, G. Infrared Thermography for the Evaluation of Inflammatory and Degenerative Joint Diseases: A Systematic Review. *Cartilage* **2021**, *13*, 1790s–1801s. [CrossRef] [PubMed]
22. Vardasca, R.; Magalhaes, C.; Silva, P.; Abreu, P.; Mendes, J.; Restivo, M.T. Biomedical musculoskeletal applications of infrared thermal imaging on arm and forearm: A systematic review. *J. Therm. Biol.* **2019**, *82*, 164–177. [CrossRef]
23. Kumar, P.; Gaurav, A.; Rajnish, R.K.; Sharma, S.; Kumar, V.; Aggarwal, S.; Patel, S. Applications of thermal imaging with infrared thermography in Orthopaedics. *J. Clin. Orthop. Trauma.* **2022**, *24*, 101722. [CrossRef]
24. Kohn, M.D.; Sassoon, A.A.; Fernando, N.D. Classifications in brief: Kellgren-Lawrence classification of osteoarthritis. *Clin. Orthop. Relat. Res.* **2016**, *474*, 1886–1893. [CrossRef]
25. Kellgren, J.H.; Lawrence, J. Radiological assessment of osteo-arthrosis. *Ann. Rheum. Dis.* **1957**, *16*, 494–502. [CrossRef]
26. Hunter, D.J.; Guermazi, A.; Lo, G.H.; Grainger, A.J.; Conaghan, P.G.; Boudreau, R.M.; Roemer, F.W. Evolution of semi-quantitative whole joint assessment of knee OA: MOAKS (MRI Osteoarthritis Knee Score). *Osteoarthr. Cartil.* **2011**, *19*, 990–1002. [CrossRef]
27. D'Agostino, M.A.; Conaghan, P.; Le Bars, M.; Baron, G.; Grassi, W.; Martin-Mola, E.; Wakefield, R.; Brasseur, J.-L.; So, A.; Backhaus, M.; et al. EULAR report on the use of ultrasonography in painful knee osteoarthritis. Part 1: Prevalence of inflammation in osteoarthritis. *Ann. Rheum. Dis.* **2005**, *64*, 1703–1709. [CrossRef]
28. Ahn, S.M.; Chun, J.H.; Hong, S.; Lee, C.K.; Yoo, B.; Oh, J.S.; Kim, Y.G. The Value of Thermal Imaging for Knee Arthritis: A Single-Center Observational Study. *Yonsei Med. J.* **2022**, *63*, 141–147. [CrossRef]
29. Cafarelli, A.; Sorriento, A.; Marola, G.; Amram, D.; Rabusseau, F.; Locteau, H.; Cabras, P.; Dumont, E.; Nakhaei, S.; Jernberger, A.; et al. Usability Assessment of Technologies for Remote Monitoring of Knee Osteoarthritis. *IEEE Open J. Eng. Med. Biol.* **2024**, *5*, 476–484. [CrossRef] [PubMed]
30. Capo, A.; Di Paolo, J.; Celletti, E.; Ismail, E.; Merla, A.; Amerio, P. Thermal alterations in patients with inflammatory diseases: A comparison between psoriatic and rheumatoid arthritis. *Reumatismo* **2018**, *70*, 225–231. [CrossRef]
31. Cerqueira, J.; Branco, C.A.; Vilaça, A.; Mendes, J. Hand Neuropathies and Musculoskeletal Disorders: Complementary Diagnosis Using IR Thermography. *Appl. Sci.* **2024**, *14*, 70. [CrossRef]
32. Dallimore, S.M.; Puli, N.; Kim, D.; Kaminski, M.R. Infrared dermal thermometry is highly reliable in the assessment of patients with Charcot neuroarthropathy. *J. Foot Ankle Res.* **2020**, *13*, 56. [CrossRef] [PubMed]
33. De Marziani, L.; Boffa, A.; Orazi, S.; Andriolo, L.; Di Martino, A.; Zaffagnini, S.; Filardo, G. Joint Response to Exercise Is Affected by Knee Osteoarthritis: An Infrared Thermography Analysis. *J. Clin. Med.* **2023**, *12*, 3399. [CrossRef] [PubMed]
34. Gatt, A.; Mercieca, C.; Borg, A.; Grech, A.; Camilleri, L.; Gatt, C.; Chockalingam, N.; Formosa, C. A comparison of thermographic characteristics of the hands and wrists of rheumatoid arthritis patients and healthy controls. *Sci. Rep.* **2019**, *9*, 17204. [CrossRef]
35. Gatt, A.; Mercieca, C.; Borg, A.; Grech, A.; Camilleri, L.; Gatt, C.; Chockalingam, N.; Formosa, C. Thermal characteristics of rheumatoid feet in remission: Baseline data. *PLoS ONE* **2020**, *15*, e0243078. [CrossRef] [PubMed]
36. Gizinska, M.; Rutkowski, R.; Szymczak-Bartz, L.; Romanowski, W.; Straburzynska-Lupa, A. Thermal imaging for detecting temperature changes within the rheumatoid foot. *J. Therm. Anal. Calorim.* **2021**, *145*, 77–85. [CrossRef]
37. Gunay, H.; Bakan, O.M.; Mirzazade, J.; Sozbilen, M.C. A New Perspective on the Diagnosis of Septic Arthritis: High-Resolution Thermal Imaging. *J. Clin. Med.* **2023**, *12*, 1573. [CrossRef]
38. Ihnatouski, M.; Pauk, J.; Daunoraviciene, K.; Ziziene, J. Comparing the Heating Rate of the Proximal Phalanx of the Fingers in Rheumatoid Arthritis and Healthy Subjects. *Acta Mech. Autom.* **2024**, *18*, 490–495. [CrossRef]
39. Jones, B.; Hassan, I.; Tsuyuki, R.T.; Dos Santos, M.F.; Russell, A.S.; Yacyshyn, E. Hot joints: Myth or reality? A thermographic joint assessment of inflammatory arthritis patients. *Clin. Rheumatol.* **2018**, *37*, 2567–2571. [CrossRef] [PubMed]
40. Lerkvaleekul, B.; Jaovisidha, S.; Sungkarat, W.; Chitrapazt, N.; Fuangfa, P.; Ruangchaijatuporn, T.; Vilaiyuk, S. The comparisons between thermography and ultrasonography with physical examination for wrist joint assessment in juvenile idiopathic arthritis. *Physiol. Meas.* **2017**, *38*, 691–700. [CrossRef]

41. Lohchab, V.; Rathod, P.; Mahapatra, P.K.; Bachhal, V.; Hooda, A. Non-invasive assessment of knee osteoarthritis patients using thermal imaging. *IET Sci. Meas. Technol.* **2022**, *16*, 242–249. [CrossRef]
42. Nath, S.; Das, K.; Bhowmik, M.K. Role of Infrared Imaging for Detection of Subclinical Inflammation of Joints: A Prospective Cohort Study. *J. Clin. Diagn. Res.* **2022**, *16*, KC8–KC12. [CrossRef]
43. Nwaizu, H.; Saatchi, R.; Hawley, D.P.; Ward, O. Thermal and Visual Imaging to Assist with Juvenile Idiopathic Arthritis Examination of the Knees. *Technologies* **2020**, *8*, 30. [CrossRef]
44. Pauk, J.; Ihnatouski, M.; Wasilewska, A. Detection of inflammation from finger temperature profile in rheumatoid arthritis. *Med. Biol. Eng. Comput.* **2019**, *57*, 2629–2639. [CrossRef]
45. Siddiqui, M.A.; Baskın, E.; Yavuz Çolak, M. Pediatric Joint Inflammation Detection Using Smartphone-Based Infrared Thermography: A Prospective Study. *Clin. Pediatr.* **2025**, *64*, 1589–1597. [CrossRef]
46. Silva, N.C.D.O.V.E.; Anjos, R.L.D.; Santana, M.M.C.; Battistella, L.R.; Alfieri, F.M. Discordance between radiographic findings, pain, and superficial temperature in knee osteoarthritis. *Reumatologia* **2021**, *58*, 375–380. [CrossRef]
47. Tan, Y.; Lim, G.H. Assessment of joint inflammation at the wrist of patients with rheumatoid arthritis: Thermography findings closely mirror those from ultrasonography. *Clin. Exp. Rheumatol.* **2024**, *42*, 1051–1056. [CrossRef]
48. Tan, Y.K.; Conaghan, P.G. Understanding the use of thermography and its ability to predict ultrasound-detected joint inflammation at the metacarpophalangeal joint in patients with rheumatoid arthritis. *Scand. J. Rheumatol.* **2026**, *55*, 46–50. [CrossRef]
49. Tan, Y.K.; Hong, C.; Li, H.; Allen, J.C., Jr.; Thumboo, J. Thermography in rheumatoid arthritis: A comparison with ultrasonography and clinical joint assessment. *Clin. Radiol.* **2020**, *75*, 963.e17–963.e22. [CrossRef]
50. Tan, Y.K.; Hong, C.; Li, H.; Allen, J.C.; Thumboo, J. A novel use of combined thermal and ultrasound imaging in detecting joint inflammation in rheumatoid arthritis. *Eur. J. Radiol.* **2021**, *134*, 109421. [CrossRef] [PubMed]
51. Tan, Y.K.; Hong, C.; Li, H.; Allen, J.C.; Thumboo, J. A novel combined thermography and clinical joint assessment approach discriminates ultrasound-detected joint inflammation severity in rheumatoid arthritis at more joint sites compared to thermography alone. *Int. J. Rheum. Dis.* **2022**, *25*, 1344–1347. [CrossRef] [PubMed]
52. Tan, Y.K.; Lim, G.H. Subclinical joint inflammation in rheumatoid arthritis: Comparing thermal and ultrasound imaging at the metacarpophalangeal joint. *Adv. Rheumatol.* **2024**, *64*, 36. [CrossRef]
53. Tan, Y.K.; Lim, G.H. Comparing thermographic heat signatures with joint inflammation detected by ultrasound at the knees in patients with rheumatoid arthritis. *Sci. Rep.* **2025**, *15*, 31960. [CrossRef]
54. Tan, Y.K.; Lim, G.H.; Ooi, C.C.; Ma, V.C.; Vora, B.M.K. Thermographic and ultrasound assessment in patients with rheumatoid arthritis: Can thermography detect subclinical synovitis at the wrist? *BMC Rheumatol.* **2024**, *8*, 62. [CrossRef]
55. Tan, Y.K.; Sultana, R.; Thumboo, J. Thermography at the Elbow Among Patients with Rheumatoid Arthritis: A Comparison with Ultrasound-Detected Joint Inflammation Findings. *Rheumatol. Ther.* **2024**, *11*, 475–485. [CrossRef]
56. Tan, Y.K.; Thumboo, J. Understanding Ultrasound Power Doppler Synovitis at Clinically Quiescent Joints and Thermographic Joint Inflammation Assessment in Patients with Rheumatoid Arthritis. *Diagnostics* **2024**, *14*, 2384. [CrossRef]
57. Tu, J.F.; Wang, X.Z.; Yan, S.Y.; Wang, Y.R.; Yang, J.W.; Shi, G.X.; Zhang, W.Z.; Jin, L.N.; Yang, L.S.; Liu, D.H.; et al. Thermal sensitization of acupoints in patients with knee osteoarthritis: A cross-sectional case-control study. *J. Integr. Med.* **2025**, *23*, 289–296. [CrossRef]
58. Ugur, S.; Irim, Y.; Yücel, A.A.; Carlak, H.F.; Kaçar, C. A comparison of thermal characteristics of the small joints of the hands between patients with rheumatoid arthritis and healthy controls. *Arch. Rheumatol.* **2024**, *39*, 617–623. [CrossRef]
59. Vasdev, V.; Singh, R.; Aggarwal, V.; Bhatt, S.; Kartik, S.; Hegde, A.; Kumar, A.; Bhaskar, S.V. Thermal imaging in rheumatoid arthritis knee joints and its correlation with power Doppler ultrasound. *Med. J. Armed Forces India* **2023**, *79*, S189–S195. [CrossRef] [PubMed]
60. Zhao, Y.; Iyer, R.S.; Thapa, M.; Biswas, D.; Bhide, N.; Scheck, J.; Cain, K.; Partridge, S.C.; Wallace, C.A. A Novel Algorithm Using Within-leg Calibration for Enhanced Accuracy of Detection of Arthritis by Infrared Thermal Imaging in Children. *J. Rheumatol.* **2022**, *49*, 81–88. [CrossRef] [PubMed]
61. Ahalya, R.K.; Almutairi, F.M.; Snekhalatha, U.; Dhanraj, V.; Aslam, S.M. RANet: A custom CNN model and quanvolutional neural network for the automated detection of rheumatoid arthritis in hand thermal images. *Sci. Rep.* **2023**, *13*, 15638. [CrossRef] [PubMed]
62. Ahalya, R.K.; Snekhalatha, U.; Dhanraj, V. Automated segmentation and classification of hand thermal images in rheumatoid arthritis using machine learning algorithms: A comparison with quantum machine learning technique. *J. Therm. Biol.* **2023**, *111*, 103404. [CrossRef]
63. Bardhan, S.; Bhowmik, M.K. 2-Stage classification of knee joint thermograms for rheumatoid arthritis prediction in subclinical inflammation. *Australas. Phys. Eng. Sci. Med.* **2019**, *42*, 259–277. [CrossRef]
64. Bardhan, S.; Bhowmik, M.K.; Debnath, T.; Bhattacharjee, D. RASIT: Region shrinking based Accurate Segmentation of Inflammatory areas from Thermograms. *Biocybern. Biomed. Eng.* **2018**, *38*, 903–917. [CrossRef]

65. Carlak, H.F.; Irim, Y.; Ugur, S.; Kaçar, C.; Yücel, A.A. A method for the assessment of rheumatoid arthritis using neural network supported static and dynamic thermal analysis. *Phys. Eng. Sci. Med.* 2026, *in press*. [CrossRef]
66. Das, K.; Bhowmik, M.K.; Chowdhuary, O.; Bhattacharjee, D.; De, B.K. Accurate segmentation of inflammatory and abnormal regions using medical thermal imagery. *Australas. Phys. Eng. Sci. Med.* **2019**, *42*, 647–657. [CrossRef] [PubMed]
67. Das, K.; Debnath, R.; Bhowmik, M.K. Cluster ensemble based semi supervised ROI segmentation in thermal images. *Biomed. Signal Process. Control* **2026**, *113*, 108931. [CrossRef]
68. Das, P.; Nath, S.; Gupta, R.; Roy, S.D.; Bhowmik, M.K. Infrared thermogram image guided discontinuous appearances of hyaluronic acid for classification of arthritic knee joints. *J. Therm. Biol.* **2024**, *123*, 103915. [CrossRef]
69. Kesavapillai, A.R.; Aslam, S.M.; Umapathy, S.; Almutairi, F. RA-XTNet: A Novel CNN Model to Predict Rheumatoid Arthritis from Hand Radiographs and Thermal Images: A Comparison with CNN Transformer and Quantum Computing. *Diagnostics* **2024**, *14*, 1911. [CrossRef]
70. Ma, B.T.; Chen, J.J.; Yan, X.X.; Cheng, Z.Z.; Qian, N.F.; Wu, C.Y.; Sun, W.Q. Objectively assessing visual analogue scale of knee osteoarthritis pain using thermal imaging. *Displays* **2024**, *84*, 102770. [CrossRef]
71. Morales-Ivorra, I.; Narváez, J.; Gómez-Vaquero, C.; Moragues, C.; Nolla, J.M.; Narváez, J.A.; Marín-López, M.A. Assessment of inflammation in patients with rheumatoid arthritis using thermography and machine learning: A fast and automated technique. *RMD Open* **2022**, *8*, e002458. [CrossRef]
72. Morales-Ivorra, I.; Narváez, J.; Gómez-Vaquero, C.; Moragues, C.; Nolla, J.M.; Narváez, J.A.; Marín-López, M.A. A Thermographic Disease Activity Index for remote assessment of rheumatoid arthritis. *RMD Open* **2022**, *8*, e002615. [CrossRef]
73. Morales-Ivorra, I.; Taverner, D.; Codina, O.; Castell, S.; Fischer, P.; Onken, D.; Martínez-Osuna, P.; Battioui, C.; Marín-López, M.A. External Validation of the Machine Learning-Based Thermographic Indices for Rheumatoid Arthritis: A Prospective Longitudinal Study. *Diagnostics* **2024**, *14*, 1394. [CrossRef] [PubMed]
74. Pauk, J.; Trinkunas, J.; Puronaite, R.; Ihnatouski, M.; Wasilewska, A. A computational method to differentiate rheumatoid arthritis patients using thermography data. *Technol. Health Care* **2022**, *30*, 209–216. [CrossRef]
75. Rudnicka, Z.; Pauk, K.; Pauk, J.; Ihnatouski, M.; Pregowska, A. Energy-efficient detection of rheumatoid arthritis using spiking neural networks and thermographic imaging. *Biocybern. Biomed. Eng.* **2026**, *46*, 266–277. [CrossRef]
76. Snekhalatha, U.; Rajalakshmi, T.; Gopikrishnan, M.; Gupta, N. Computer-based automated analysis of X-ray and thermal imaging of knee region in evaluation of rheumatoid arthritis. *Proc. Inst. Mech. Eng. Part H—J. Eng. Med.* **2017**, *231*, 1178–1187. [CrossRef]
77. Umapathy, S.; Thulasi, R.; Gupta, N.; Sivanadhan, S. Thermography and colour Doppler ultrasound: A potential complementary diagnostic tool in evaluation of rheumatoid arthritis in the knee region. *Biomed. Eng.-Biomed. Tech.* **2020**, *65*, 289–299. [CrossRef]
78. Umapathy, S.; Vasu, S.; Gupta, N. Computer Aided Diagnosis Based Hand Thermal Image Analysis: A Potential Tool for the Evaluation of Rheumatoid Arthritis. *J. Med. Biol. Eng.* **2018**, *38*, 666–677. [CrossRef]
79. Ghosh, J.; Singh, R.; Rastogi, A. Infrared Dermal Thermometry in Active Charcot Neuro-Osteoarthropathy of Foot. *Indian J. Endocrinol. Metab.* **2025**, *29*, 303–307. [CrossRef]
80. Armstrong, D.G.; Lavery, L.A.; Liswood, P.J.; Todd, W.F.; Tredwell, J.A. Infrared Dermal Thermometry for the High-Risk Diabetic Foot. *Phys. Ther.* **1997**, *77*, 169–175. [CrossRef] [PubMed]
81. Lin, S.J.; Chang, F.C.; Huang, T.W.; Peng, K.T.; Shih, H.N.; Lee, M.S. Temporal Change of Interleukin-6, C-Reactive Protein, and Skin Temperature after Total Knee Arthroplasty Using Triclosan-Coated Sutures. *BioMed Res. Int.* **2018**, *2018*, 9136208. [CrossRef]
82. Zampeli, E.; Raftakis, I.; Michelongona, A.; Nikolaou, C.; Elezoglou, A.; Toutouzas, K.; Siores, E.; Sfikakis, P.P. Detection of subclinical synovial inflammation by microwave radiometry. *PLoS ONE* **2013**, *8*, e64606. [CrossRef]
83. Verstockt, J.; Verspeek, S.; Thiessen, F.; Tjalma, W.A.; Brochez, L.; Steenackers, G. Skin Cancer Detection Using Infrared Thermography: Measurement Setup, Procedure and Equipment. *Sensors* **2022**, *22*, 3327. [CrossRef]
84. Tan, Y.K.; Hong, C.; Li, H.; Allen, J.C., Jr.; Thumboo, J. Receiver operating characteristic analysis using a novel combined thermal and ultrasound imaging for assessment of disease activity in rheumatoid arthritis. *Sci. Rep.* **2022**, *12*, 22115. [CrossRef] [PubMed]
85. Pauk, J.; Wasilewska, A.; Ihnatouski, M. Infrared thermography sensor for disease activity detection in rheumatoid arthritis patients. *Sensors* **2019**, *19*, 3444. [CrossRef]
86. Wong, S.; Bhide, N.; Balay-Dustrude, E.; Sullivan, E.; Scheck, J.; Muse, I.; Cain, K.; Biswas, D.; Partridge, S.C.; Zhao, Y. Feasibility of applying infrared thermal imaging for home monitoring of arthritis in children. *Pediatr. Rheumatol. Online J.* **2025**, *23*, 84. [CrossRef]
87. Pelechas, E.; Kaltsonoudis, E.; Voulgari, P.V.; Drosos, A.A. Psoriatic Arthritis. In *Illustrated Handbook of Rheumatic and Musculo-Skeletal Diseases*; Pelechas, E., Kaltsonoudis, E., Voulgari, P.V., Drosos, A.A., Eds.; Springer International Publishing: Cham, Switzerland, 2023; pp. 195–225. [CrossRef]
88. Embaby, O.; Bin Asmadi, A.; Binte Asmadi, A.; Haroun, A.; Mersal, M.; Elalfy, M. Pathogenesis of Acute Diabetic Charcot Arthropathy in the Foot and Ankle: A Comprehensive Literature Review. *Orthop. Rev.* **2025**, *17*, 144007. [CrossRef] [PubMed]
89. Windisch, C.; Brodt, S.; Roehner, E.; Matziolis, G. Regional differences in temperature course after knee arthroplasty. *Knee Surg. Sports Traumatol. Arthrosc.* **2016**, *24*, 2686–2691. [CrossRef]

90. Sharma, R. Skin Temperature Following Total Knee Arthroplasty: A Longitudinal Observational Study. *J. Arthroplast.* **2024**, *39*, 2466–2470. [CrossRef] [PubMed]
91. Petrigna, L.; Amato, A.; Roggio, F.; Trovato, B.; Musumeci, G. Thermal threshold for knee osteoarthritis people evaluated with infrared thermography: A scoping review. *J. Therm. Biol.* **2024**, *123*, 103932. [CrossRef]
92. Cristea, S.; Predescu, V.; Dragosloveanu, Ş.; Cuculici, Ş.; Marandici, N. Surgical Approaches for Total Knee Arthroplasty. In *Arthroplasty—A Comprehensive Review*; Bagaria, V., Ed.; IntechOpen: London, UK, 2016. [CrossRef]
93. Calin, M.A.; Mologhianu, G.; Savastru, R.; Calin, M.R.; Brailescu, C.M. A review of the effectiveness of thermal infrared imaging in the diagnosis and monitoring of knee diseases. *Infrared Phys. Technol.* **2015**, *69*, 19–25. [CrossRef]
94. Gavish, L.; Kandel, L.; Rivkin, G.; Gertz, S.D.; Hoffer, O. Natural history of changes in knee skin temperature following total knee arthroplasty: A systematic review and meta-analysis. *Sci. Rep.* **2023**, *13*, 6810. [CrossRef]
95. Slomka, B.; Rongies, W.; Ruszczuk, P.; Sierdzinski, J.; Saganowska, D.; Zdunski, S.; Worwag, M.E. Short-term effect of kinesiology taping on temperature distribution at the site of application. *Res. Sports Med.* **2018**, *26*, 365–380. [CrossRef]
96. der Strasse, W.A.; Campos, D.P.; Mendonça, C.J.A.; Soni, J.F.; Mendes, J.; Nohama, P. Detecting bone lesions in the emergency room with medical infrared thermography. *Biomed. Eng. Online* **2022**, *21*, 35. [CrossRef]
97. Gorecki, G.P.; Tomescu, D.R.; Pleș, L.; Panaitescu, A.M.; Dragosloveanu, Ș.; Scheau, C.; Sima, R.M.; Coman, I.S.; Grigorean, V.T.; Cochior, D. Implications of using artificial intelligence in the diagnosis of sepsis/sepsis shock. *Germs* **2024**, *14*, 77–84. [CrossRef]
98. Abins, T.; Veluguleti, U.; Sheenam, N.; Kumar, S.; Gaur, N.; Gosh, A.; Hussain, R.; Gonnade, N.; Gaur, R.; Sarankumar, G. Association Between Systemic Inflammation and Radiographic Severity in Knee Osteoarthritis: A Trial Baseline Cohort Analysis. *Cureus* **2025**, *17*, 93371. [CrossRef]
99. Tankala, J.; Parameswaran, A.; Yadav, V.K.; Nori, M.; Eachempati, K.K.; Apsingi, S. Asymptomatic rotator cuff tears among the indian population: Prevalence, risk factors, and tear characteristics. *Indian J. Orthop.* **2025**, *59*, 800–806. [CrossRef]
100. Rowe, G.S.; Blazevich, A.J.; Taylor, J.L.; Pulverenti, T.; Haff, G.G. Can the cross-education of strength attenuate the impact of detraining after a period of strength training? A quasi-randomized trial. *Eur. J. Appl. Physiol.* **2024**, *124*, 1–16. [CrossRef]
101. Ilo, A.; Romsi, P.; Mäkelä, J. Infrared thermography and vascular disorders in diabetic feet. *J. Diabetes Sci. Technol.* **2020**, *14*, 28–36. [CrossRef]
102. Staffa, E.; Bernard, V.; Kubicek, L.; Vlachovsky, R.; Vlk, D.; Mornstein, V.; Bourek, A.; Staffa, R. Infrared thermography as option for evaluating the treatment effect of percutaneous transluminal angioplasty by patients with peripheral arterial disease. *Vascular* **2017**, *25*, 42–49. [CrossRef]
103. Lim, M.J.; Kwon, S.R.; Jung, K.-H.; Joo, K.; Park, S.-G.; Park, W. Digital thermography of the fingers and toes in Raynaud's phenomenon. *J. Korean Med. Sci.* **2014**, *29*, 502. [CrossRef]
104. Huang, L.; Chen, Z.; Yang, Z.; Huang, W. Advancing healthcare accessibility: Fusing artificial intelligence with flexible sensing to forge digital health innovations. *BME Front.* **2024**, *5*, 0062. [CrossRef]
105. Dragosloveanu, S.; Vulpe, D.E.; Andrei, C.A.; Nedelea, D.G.; Garofil, N.D.; Anghel, C.; Dragosloveanu, C.D.M.; Cergan, R.; Scheau, C. Predicting periprosthetic joint Infection: Evaluating supervised machine learning models for clinical application. *J. Orthop. Transl.* **2025**, *54*, 51–64. [CrossRef] [PubMed]
106. Vulpe, D.E.; Anghel, C.; Scheau, C.; Dragosloveanu, S.; Săndulescu, O. Artificial Intelligence and Its Role in Predicting Periprosthetic Joint Infections. *Biomedicines* **2025**, *13*, 1855. [CrossRef] [PubMed]
107. Samadi, N.; Thapa, D.; Salimi, M.; Parkhimchyk, A.; Tabatabaei, N. Low-Cost Active Thermography using Cellphone Infrared Cameras: From Early Detection of Dental Caries to Quantification of THC in Oral Fluid. *Sci. Rep.* **2020**, *10*, 7857. [CrossRef] [PubMed]